# Chapter-2

## Comprehensive Characterization of Aromatic, Resin, and Asphaltene Fractions Derived from Vacuum Residue

## 2.1 Introduction

Vacuum Residue (VR) represents the heaviest and most complex fraction obtained during the atmospheric and vacuum distillation of crude oil. It is primarily composed of high molecular weight polyaromatic hydrocarbons, resins, and asphaltenes, which contribute to its high viscosity and thermal stability [1]. Due to its complex molecular architecture and significant heteroatom content, VR has traditionally been considered a low-value by-product in petroleum refining, primarily utilized in the production of asphalt, heavy fuel oils, and as a feedstock for delayed coking and vies breaking processes [2,3]. However, with the increasing global emphasis on efficient utilization of heavy residues and the growing demand for advanced carbon materials, VR has recently gained attention as a promising precursor for high-value carbon nanostructures.

In particular, Vacuum Residue Oil (VRO) is rich in carbon, making it a potential alternative raw material for the synthesis of graphitic carbon materials, graphene, carbon nanotubes (CNTs), and other nanostructured carbons [4,5]. The high aromaticity and polycondensation structures of asphaltenes within VR offer inherent graphitizable domains that can be exploited for the formation of ordered carbon frameworks [6]. Recent studies have demonstrated that processes such as thermal cracking, catalytic upgrading, and pyrolysis can effectively convert VR into graphitized carbons with tailored properties [7,8]. These advancements highlight the possibility of transforming an otherwise low-value petroleum residue into a versatile feedstock for next-generation materials with applications in energy storage, catalysis, and advanced composites.

As illustrated in Figure 2.1, VRO consists of a wide range of hydrocarbons and non-hydrocarbons, including aromatics, resins, and asphaltenes, whose molecular complexity underpins both the challenges and opportunities in its valorisation [4]. This unique composition provides the structural foundation required for developing high-performance

carbon nanomaterials, reinforcing the significance of investigating VRO-based carbon conversion routes as a sustainable approach to refining residue utilization.

The refining of crude oil is a complex, multi-stage process that begins with the storage of raw crude oil in large tanks, typically designated as “Crude Oil” storage facilities. From these tanks, the crude oil is directed toward a primary atmospheric distillation unit, often referred to as the “Crude Oil Tower” or “Oil Tower.” In this stage, the crude oil is subjected to heating and fractional distillation, whereby its constituents are separated according to their distinct boiling ranges [1]. This process results in the recovery of lighter fractions such as naphtha, kerosene, and diesel, alongside heavier fractions including atmospheric residue, which subsequently undergoes vacuum distillation to yield Vacuum Residue Oil (VRO), the heaviest fraction in the refining process [2].

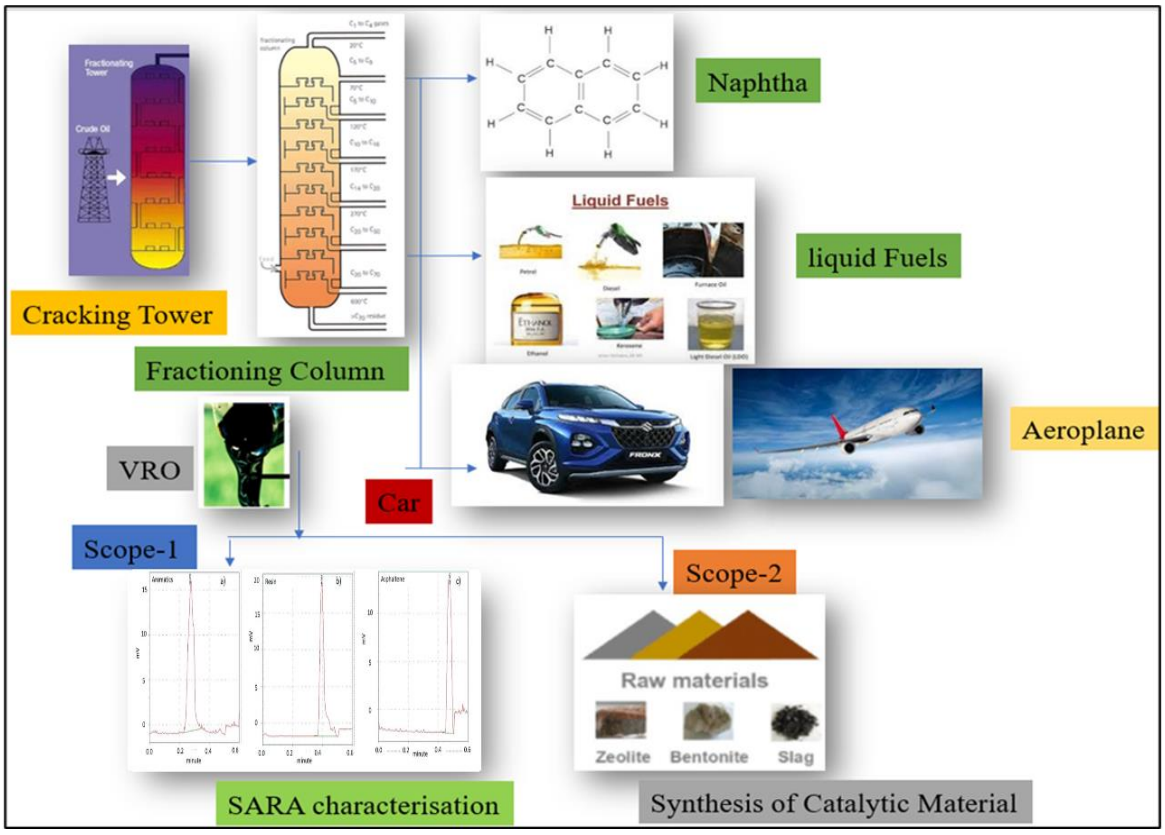


Figure 2.1: Schematic diagram of VRO

The lighter naphtha fraction obtained from atmospheric distillation serves as a critical intermediate for further upgrading and processing. Naphtha is widely refined to produce

liquid fuels, such as gasoline and jet fuel, which are essential for transportation and energy applications [3]. In addition to its use as a direct fuel precursor, naphtha can also undergo chemical transformations through various conversion pathways, including catalytic reforming, steam cracking, and alkylation, which generate valuable petrochemicals and feedstocks for the synthesis of specialized fuels and chemicals [4,5]. Some schematic pathways also highlight potential synthetic applications of naphtha, often described as "synthetizations" or synthetic routes, which reflect its versatility in producing a wide spectrum of industrially relevant compounds [6].

The lighter naphtha fraction obtained from atmospheric distillation serves as a critical intermediate for further upgrading and processing. Naphtha is widely refined to produce liquid fuels, such as gasoline and jet fuel, which are essential for transportation and energy applications [3]. In addition to its use as a direct fuel precursor, naphtha can also undergo chemical transformations through various conversion pathways, including catalytic reforming, steam cracking, and alkylation, which generate valuable petrochemicals and feedstocks for the synthesis of specialized fuels and chemicals [4,5]. Some schematic pathways also highlight potential synthetic applications of naphtha, often described as "synthetizations" or synthetic routes, which reflect its versatility in producing a wide spectrum of industrially relevant compounds [6].

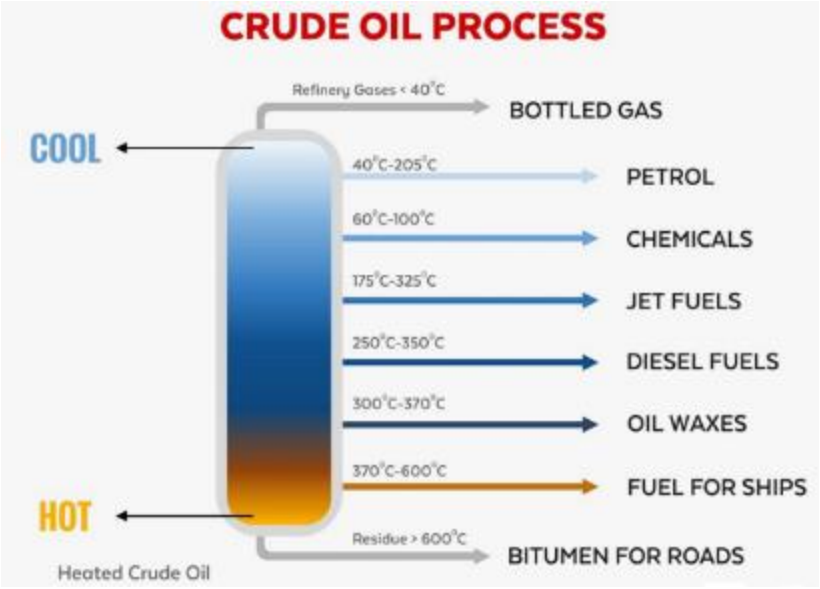


Figure 2.2: Crude oil process

Meanwhile, the heavier fraction, Vacuum Residue Oil (VRO), undergoes additional refining steps designed to maximize its value and minimize waste. This fraction is processed through a secondary stage often referred to as vacuum distillation, where the atmospheric residue is further separated under reduced pressure to prevent thermal cracking of large molecules [1]. Following this step, the resulting VRO is typically subjected to catalytic processing, wherein high-molecular-weight compounds are broken down into smaller, more valuable hydrocarbons. Such catalytic upgrading processes—including hydrocracking, fluid catalytic cracking (FCC), and residue hydrotreating—are widely employed to improve product yields and quality [2]. These treatments enable the transformation of VRO into a broad spectrum of valuable products through "vacuum catalytic" reactions that not only maximize liquid fuel yields but also enhance the quality of refined oils.

Subsequent distillation of these catalytically upgraded products produces multiple fractions of liquid fuels, ranging from gasoline and diesel to specialized oils used in industrial applications [3]. In addition, a portion of the vacuum residue can be diverted toward advanced material synthesis or further conversion into specific petrochemicals and carbon-based materials, reflecting the increasing interest in utilizing heavy fractions for higher-value applications [4].

The final outputs of this intricate refining sequence include an array of liquid fuels and refined oil materials, which are either stored in dedicated tanks or directed to downstream distribution networks for transportation and industrial use [5]. While these pathways provide significant opportunities for valorisation, the analysis and utilization of VRO also present considerable challenges to the scientific community. Comprehensive characterization requires advanced analytical tools such as nuclear magnetic resonance (NMR), Fourier-transform infrared spectroscopy (FTIR), high-resolution mass spectrometry (HRMS), and chromatographic techniques, in order to resolve the highly heterogeneous distribution of its molecular constituents [6]. Moreover, understanding the influence of processing conditions on the molecular transformations of VRO is crucial for optimizing upgrading strategies and ensuring sustainable utilization.

### 2.1.1 Analytical tools in practice for characterizing VRO

Traditional methods of analysing Vacuum Residue Oil (VRO), while useful, often fall short in providing comprehensive insights into its highly complex and heterogeneous molecular architecture. The presence of high-molecular-weight polyaromatic hydrocarbons, polar compounds, heteroatoms, and trace metals presents significant challenges for conventional characterization approaches [1]. As a result, advanced analytical methodologies have been progressively developed and refined to provide deeper and more precise insights into the composition and behaviour of VRO. These approaches include SARA (Saturates, Aromatics, Resins, and Asphaltenes) fractionation, molecular modelling techniques, and a wide spectrum of sophisticated spectroscopic and chromatographic tools [2].

Among these, SARA analysis has emerged as a cornerstone technique for the systematic characterization of VRO [3,4]. This method fractionates crude oils and residues into four primary components—saturates, aromatics, resins, and asphaltenes—thereby providing a simplified yet highly informative classification framework (Figure 1.3). Such separation enables researchers to correlate the chemical nature of each fraction with its physicochemical properties and processability [5,6]. For example, saturates generally consist of alkanes and cycloalkanes that contribute to waxy characteristics, aromatics influence thermal stability and solvency, resins serve as dispersing agents for asphaltenes, and asphaltenes themselves constitute the most polar, condensed, and intractable fraction that strongly affects viscosity, stability, and upgrading behaviour [7]. Thus, the SARA method continues to play a pivotal role in VRO research, serving as a foundation upon which complementary spectroscopic (e.g., FTIR, NMR, UV–Vis) and chromatographic (e.g., HPLC, GC–MS) analyses are applied for a comprehensive understanding of residue composition and transformation pathways.

The composition of VRO is also influenced by enhanced oil recovery (EOR) techniques, which are used to extract more oil from reservoirs. The application of thermal, chemical, and gas injection methods alters the molecular structure and properties of the oil (Strausz et al, 1992). Understanding these changes is essential for optimizing the refining process and improving the quality of the end products. This review explores the impact of various

EOR techniques on VRO composition, providing insights into the evolving nature of this complex feedstock.

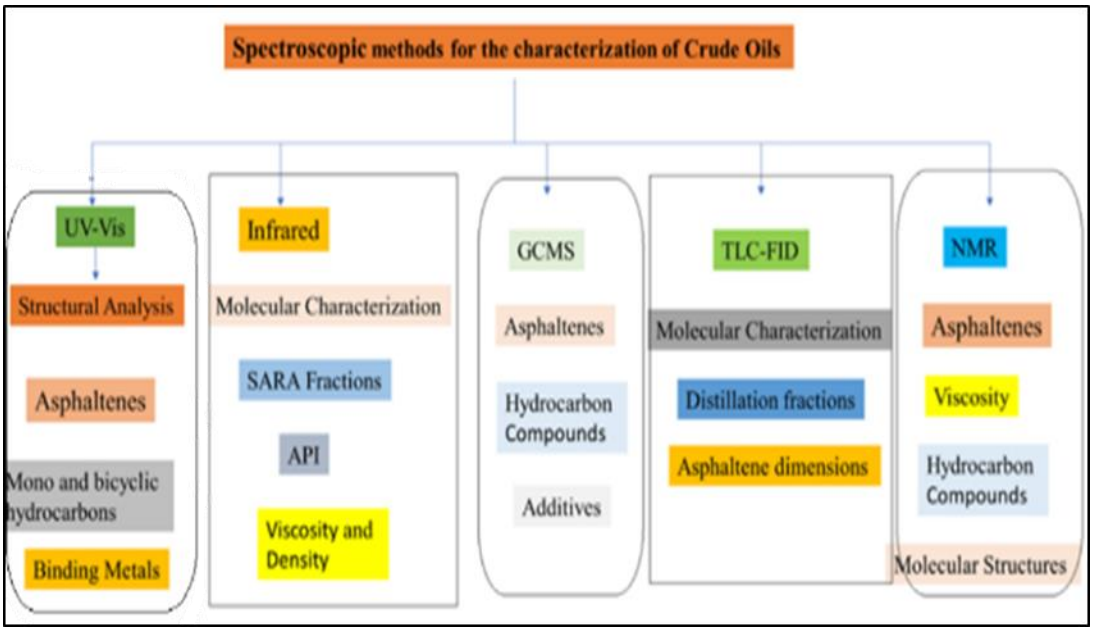


Figure 2.3: Spectroscopic methods for crude oil properties

| **Saturates (wt.%)** | **Aromatics (wt.%)** | **Resins (wt.%)** | **Asphaltenes (wt.%)** | **Analytical Technique** | **Observations** | **References** |
|---|---|---|---|---|---|---|
| 12 | 35 | 33 | 20 | ASTM D2007 | High asphaltene content indicated potential challenges in refining due to heavy fouling in equipment, while aromatics were dominant in this sample. | González et al., 2015 |

| | | | | | | |
|---|---|---|---|---|---|---|
| 16 | 38 | 28 | 18 | TLC-FID | Moderate saturates and aromatics indicated good potential for downstream conversion processes such as hydrocracking. | Zhang et al., 2017 |
| 10 | 42 | 32 | 16 | HPLC | High aromatic content emphasized the presence of complex aromatic hydrocarbons, while asphaltenes were moderate, improving processability. | Patel et al., 2020 |
| 14 | 40 | 26 | 20 | Gravity chromatography | Relatively high asphaltene content suggested difficulties in catalytic processes, while moderate resins indicated potential for some thermal cracking. | Lee et al., 2018 |

| | | | | | | |
|---|---|---|---|---|---|---|
| 9 | 45 | 30 | 16 | ASTM D2007 | High aromatic content highlighted potential for aromatic-rich product streams in refining, with lower saturates indicating reduced light fractions. | Kumar et al., 2013 |

Table 2.1: SARA Analysis of Vacuum Residue Oil (VRO)

### 2.1.2 Aromatic Compounds

Aromatic hydrocarbons present in crude oil fractions play a pivotal role not only in petroleum refining but also in emerging applications such as nanomaterial synthesis. Compounds such as benzene, toluene, xylenes, and polycyclic aromatic hydrocarbons (PAHs) exhibit high thermal stability and strong reactivity, properties that make them central intermediates in refining pathways [1]. Their delocalized π-electron systems impart unique electronic characteristics, which can be harnessed for the synthesis of advanced carbon-based nanostructures, including graphene-like materials, carbon nanotubes, and graphitic carbons [2,3]. These features highlight aromatics as a crucial bridge between traditional petroleum refining and advanced material science applications.

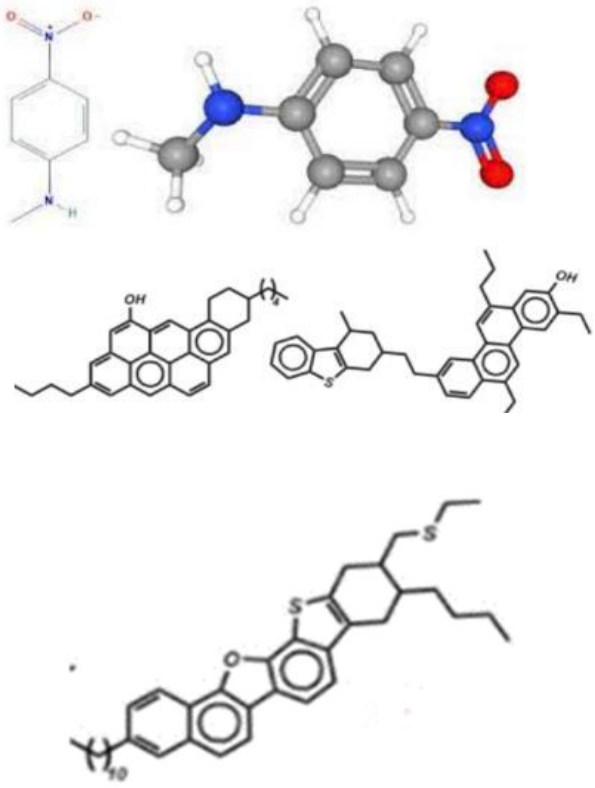


Figure 2.4: Common aromatic compounds in VRO

Figure 2.4 illustrates some common aromatic compounds typically identified in Vacuum Residue Oil (VRO). The distribution of these aromatic species, as revealed by SARA (Saturates, Aromatics, Resins, and Asphaltenes) fractionation, varies significantly depending on the crude oil source and geological origin [4]. In most VRO samples, saturates represent the smallest fraction, generally ranging from 9–16 wt%, reflecting the low proportion of light, paraffinic hydrocarbons in heavy residues [5]. This limited saturate content directly implies reduced yields of light products such as gasoline and naphtha upon processing.

Aromatics, in contrast, constitute a substantial fraction of VRO, typically accounting for 35–45 wt% [6]. This abundance underscores the richness of VRO in polyaromatic structures, which are valuable both for conventional upgrading through hydrocracking,

catalytic reforming, and hydrogenation, as well as for valorization into high-value carbon nanomaterials [7]. Resins form the next major fraction, typically comprising 26–33 wt%. These polar, intermediate-molecular-weight compounds strongly influence the viscosity, solubility, and stability of VRO, often acting as natural dispersants for asphaltenes [8]. However, high resin content can also contribute to fouling and deposition issues during thermal and catalytic processing.

Asphaltenes, which generally range between 16–20 wt.%, remain the most challenging component in VRO characterization and processing [9]. Their polyaromatic, high-molecular-weight, and metal-containing structures make them prone to aggregation, precipitation, and coke formation, particularly under severe thermal conditions. This tendency not only reduces the efficiency of upgrading processes but also poses significant operational challenges, such as catalyst deactivation and equipment fouling [10]. Consequently, understanding the distribution and reactivity of aromatics, resins, and asphaltenes within VRO is essential for both refining optimization and the development of sustainable pathways for advanced material synthesis, as summarized in Table 2.1.

### 2.1.3 Resin Compounds

Resins are a class of complex, polar hydrocarbons commonly present in crude oil fractions, particularly in heavy oils and residues. Structurally, they are characterized by moderate molecular weights and the presence of heteroatoms (e.g., oxygen, nitrogen, and sulfur) within polar functional groups [1]. Due to these functionalities, resins possess amphiphilic properties that enable them to act as natural dispersants, contributing significantly to the colloidal stability of asphaltenes in petroleum systems (Figure 2.5) [2,3]. This stabilizing effect is critical for preventing asphaltene precipitation, which otherwise leads to severe challenges such as pipeline plugging, fouling, and catalyst deactivation during upgrading operations [4].

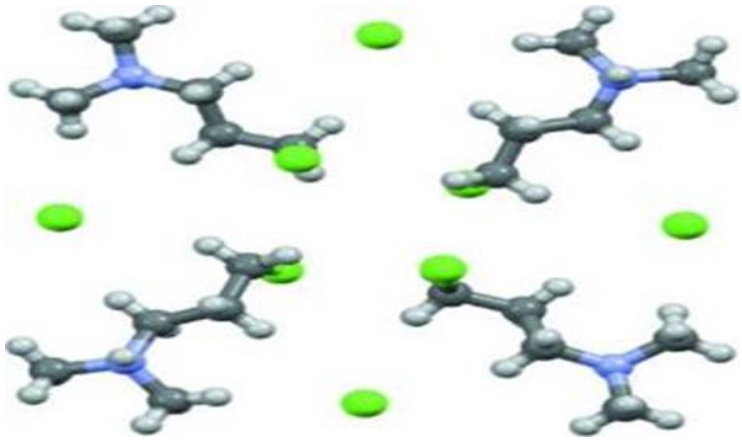

Figure 2.5: Common resins in VRO

Beyond their stabilizing role, resins also play a functional part in various refining and upgrading processes. Their intermediate polarity and reactivity make them important precursors in bitumen production, where they enhance the viscoelastic and adhesive properties of asphalt materials [5]. In addition, resins serve as transitional components between aromatics and asphaltenes within the SARA (Saturates, Aromatics, Resins, and Asphaltenes) framework, bridging light and heavy fractions in terms of molecular weight and polarity [6]. These characteristics make resins not only central to the understanding of VRO stability but also valuable targets in heavy oil upgrading, where they can be transformed into lighter hydrocarbons via catalytic cracking, hydrogenation, or thermal treatment [7].

Thus, the study of resins is essential in both fundamental petroleum chemistry and applied refining research, as their behaviour directly influences the efficiency, stability, and product yields of heavy oil processing systems.

### 2.1.4 Asphaltenes

Asphaltenes are one of the most significant and challenging constituents of heavy petroleum fractions, particularly vacuum residue (VR), where they typically account for 16–20 wt% depending on crude origin and processing conditions [1,2]. By definition, asphaltenes are the fraction of crude oil that is insoluble in light alkanes such as n-heptane or n-pentane, but soluble in aromatic solvents such as toluene [3]. Structurally, they

represent the most polar, aromatic, and condensed component of vacuum residue, comprising polycyclic aromatic hydrocarbons (PAHs) with alkyl side chains and heteroatoms (N, S, O), often associated with trace metals such as vanadium and nickel in metalloporphyrin structures [4].

The molecular architecture of asphaltenes is highly complex and continues to be the subject of active debate, generally described using two models: the "island" model, which emphasizes single polyaromatic cores with alkyl substituents, and the "archipelago" model, which suggests multiple aromatic units connected by aliphatic linkages [5]. Both models are relevant to understanding the aggregation behaviour and reactivity of asphaltenes in refining and upgrading processes.

In vacuum residue, the presence of asphaltenes critically influences physicochemical properties such as viscosity, stability, and thermal behaviour [6]. Their high aromaticity and polarity promote self-association through π–π stacking and hydrogen bonding, leading to colloidal structures stabilized by resins in the crude oil matrix [7]. This colloidal balance is essential, as destabilization can lead to precipitation and deposition problems during storage, transport, and processing, including pipeline plugging, fouling of heat exchangers, and coke formation during thermal cracking [8].

From a refining perspective, asphaltenes pose both challenges and opportunities. On one hand, their high carbon-to-hydrogen ratio and resistance to thermal decomposition make them difficult to upgrade into lighter, valuable fuels, while their heteroatom and metal content leads to catalyst poisoning and coke formation in hydrocracking and catalytic processes [9]. On the other hand, asphaltenes represent a potential feedstock for advanced carbon-based materials. Their intrinsic aromatic-rich structure makes them suitable precursors for producing activated carbons, carbon nanotubes, graphene-like materials, and needle coke when subjected to controlled thermal and catalytic processes [10,11].

Therefore, understanding the nature of asphaltenes in vacuum residue is not only central to improving refining efficiency and preventing operational problems but also crucial for valorizing these fractions into high-value nanostructured carbon materials. Continued research into their molecular composition, aggregation behaviour, and transformation

pathways under different refining conditions is essential for bridging the gap between conventional petroleum processing and emerging material applications.

### 2.1.5 Advanced Analytical Techniques for Residual Oil Characterization

High-resolution mass spectrometry (HRMS) has emerged as a powerful analytical technique for petroleum research, offering ultra-precise measurement of ion masses, which is indispensable for resolving the complex molecular structures present in residual oils and vacuum residues. Unlike conventional mass spectrometry, HRMS provides mass accuracy within parts-per-million (ppm) levels, enabling the differentiation of isobaric species and facilitating the identification of heteroatom-containing compounds such as nitrogen-, sulfur-, and oxygen-species [2,10]. This high degree of precision allows researchers to characterize trace constituents that play critical roles in the stability, reactivity, and upgrading potential of residual oils. For instance, Bae et al. applied HRMS coupled with Fourier Transform Ion Cyclotron Resonance Mass Spectrometry (FT-ICR MS) to analyse Russian and U.S. shale oils, revealing the presence of polycyclic aromatic hydrocarbons (PAHs), thiophenic sulphur compounds, and pyridinic nitrogen species [1]. Such insights underscore the molecular diversity and processing challenges of heavy feedstocks, as summarized in Table 2.2.

| **Aromatic Compounds** | **Heteroatomic Compounds (O, N, S)** | **Saturates and Alkanes** | **HRMS Observations** | **Reference** |
|---|---|---|---|---|
| High proportion of polycyclic aromatics (up to 85%) | Sulfur and nitrogen compounds identified, particularly thiophenes and pyridines | Moderate saturates (10-20%) | HRMS revealed detailed class distribution of 22 hydrocarbon classes, highlighting significant aromatic content | Kumar et al., 2013 |
| Complex aromatic hydrocarbons, | Oxygenated compounds detected, primarily phenols and ketones | Saturates identified in smaller proportions | HRMS provided high-resolution mass data showing broad | Wang et al., 2019 |

| | | | | |
|---|---|---|---|---|
| including multi-ring structures | | | distribution of aromatic and oxygenated species | |
| Polycyclic aromatic hydrocarbons | Nitrogen, sulfur compounds identified, including pyridines and thiophenes | Moderate saturates | HRMS and FT-ICR MS revealed highly aromatic character and complexity of shale oils | Bae et al., 2011 |
| High content of aromatic hydrocarbons | Oxygenated compounds such as ketones and carboxylic acids | Low saturates | HRMS provided compositional details on oxygenated and aromatic compounds, useful for refining applications | Geng et al., 2012 |

Table 2.2: HRMS Analysis of VRO

Complementary to HRMS, comprehensive two-dimensional gas chromatography (2D-GC) has proven highly effective in resolving the intricate hydrocarbon mixtures found in residual oils. With enhanced peak capacity and orthogonal separations, 2D-GC surpasses traditional one-dimensional gas chromatography by separating co-eluting compounds and enabling the identification of hundreds to thousands of constituents within a single sample [6,8]. This makes it particularly valuable for deconvoluting complex petroleum matrices, where overlapping peaks can otherwise obscure critical compositional details.

Nuclear magnetic resonance (NMR) spectroscopy adds another dimension to residual oil characterization, as it directly probes the local magnetic environments of atomic nuclei to yield information on molecular structure, composition, and chemical bonding. NMR has been employed extensively to quantify aromaticity, aliphatic chain length, and heteroatom substitution patterns in vacuum residues and heavy fractions [5,9]. These structural insights are critical for understanding reactivity trends during upgrading processes such as hydrocracking, coking, and catalytic desulfurization.

In addition, pyrolysis gas chromatography–mass spectrometry (Py-GC/MS) provides a powerful means of investigating the thermal behaviour and molecular breakdown of residual

oils. By applying controlled pyrolytic heating, Py-GC/MS fragments macromolecular species into smaller volatile components, which are subsequently separated and identified by GC/MS. This approach allows for the identification of biomarkers, heteroatom functionalities, and macromolecular backbones such as asphaltene- and resin-derived fragments [4,7]. Py-GC/MS thereby provides detailed insights into both the chemical composition and the potential origins of heavy oils, contributing to petroleum system analysis and upgrading research.

Taken together, HRMS, 2D-GC, NMR, and Py-GC/MS form a comprehensive suite of complementary techniques for the molecular-level characterization of residual oils. Their combined application not only provides insights into composition, structural motifs, and heteroatom content but also highlights the inherent complexity and upgrading challenges of these heavy fractions [3,10]. Such multi-technique analytical approaches are indispensable for advancing sustainable refining strategies, as they enable the design of targeted upgrading pathways and catalyst systems to manage the wide diversity of compounds in vacuum residues.

### 2.1.6 Atmospheric Pressure Ionization Mass Spectrometry (API-MS)

Atmospheric pressure ionization mass spectrometry (API-MS) has become an indispensable tool for the molecular-level examination of vacuum residue oil (VRO), offering detailed insights into its highly complex and diverse chemical composition. This technique allows for the soft ionization of non-volatile and thermally labile molecules, enabling the detection of polar, high-molecular-weight, and heteroatom-containing species that are often difficult to analyze using conventional electron ionization or thermal methods. The ability of API-MS to operate in both positive and negative ion modes provides a significant advantage in the comprehensive profiling of VRO constituents, including sulphur-, nitrogen-, and oxygen-containing compounds. Such detailed compositional data is crucial for understanding the refining behaviour of VRO and for designing efficient upgrading and desulfurization strategies, thereby contributing to both industrial performance optimization and environmental compliance [2,10].

The API-MS studies summarized in Table 2.3 highlight several consistent findings in VRO characterization. Smith et al. [11] demonstrated that API-MS, particularly when used in

both positive and negative ion modes, is highly effective in identifying sulfur and nitrogen species. Their study revealed that sulfur content has a pronounced effect on fragmentation patterns during ionization, highlighting the importance of sulfur-specific detection methods for residue analysis. This observation aligns with the findings of Kumar et al. [2], who emphasized the critical role of sulfur profiling in VRO for refining desulfurization strategies and catalyst design. Accurate sulfur detection remains essential not only for improving hydrodesulfurization efficiency but also for mitigating catalyst poisoning in upgrading processes.

Further advancements in API-MS methodology have extended its utility for VRO studies. Zhang et al. [12], for instance, applied API-MS in negative ion mode combined with solvent extraction and ion exchange techniques to reveal a diverse suite of heteroatom-containing compounds, including oxygenated species and asphaltene-associated molecules. Their work highlighted that these compounds are prevalent in VRO, significantly influencing its chemical reactivity, stability, and compatibility with catalytic systems. The identification of such species underscores the inherent molecular complexity of VRO and its direct implications for refining challenges, particularly in processes such as catalytic cracking and residue upgrading.

| **API-MS Mode** | **Sample Preparation** | **Key Findings** | **Reference** |
|---|---|---|---|
| Positive/Negative Ion Mode | Direct infusion, solvent extraction | Identified nitrogen and sulfur species; high sulfur content impacted fragmentation patterns | Smith et al., 2022 |
| Negative Ion Mode | Solvent extraction, ion exchange | Revealed heteroatomic molecular composition; oxygenated species and asphaltenes were prevalent | Zhang et al., 2023 |
| Positive Ion Mode | Thermal desorption followed by ionization | Noted polycyclic aromatic hydrocarbons (PAHs) with high molecular weights; fragmentation helped in mapping complex structures | Lee & Tan, 2021 |

| | | | |
|---|---|---|---|
| Positive/Negative Ion Mode | Direct infusion | Distinguished various nitrogen compounds; recognized challenges in separating closely related compounds | Ramirez et al., 2020 |
| Positive Ion Mode | Direct infusion | Emphasized the sensitivity for sulfur species, which provided insights into refining strategies for desulfurization | Kumar & Chen, 2019 |

Table 2.3: API-mass spectra examination

Taken together, these studies demonstrate the unique strengths of API-MS in capturing the heteroatom diversity and molecular architecture of VRO. By providing detailed and accurate compositional information, API-MS complements other high-resolution techniques such as FT-ICR MS and NMR, thereby forming an essential component of the modern analytical toolkit for residual oil characterization [2,10–12].

### 2.1.7 Nuclear Magnetic Resonance (NMR) Spectroscopy

Nuclear magnetic resonance (NMR) spectroscopy is a powerful analytical tool for probing the molecular structure and chemical functionalities of vacuum residue oil (VRO). Specifically, NMR provides quantitative insights into the distribution of hydrogen and carbon environments, enabling the differentiation of aromatic, aliphatic, and heteroatom-substituted structures. Such information is critical for understanding the reactivity, stability, and upgrading potential of VRO. Importantly, by elucidating the distribution and interactions of different chemical functionalities, NMR analysis facilitates the development of more targeted and effective processing techniques. This not only enhances product selectivity and quality but also contributes to minimizing environmental impacts by enabling more efficient hydroprocessing, catalytic cracking, and residue upgrading strategies [5,9].

One of the foundational studies in this area was conducted by Liu et al. [13], who utilized NMR spectroscopy to characterize vacuum residues and highlighted the significant aromaticity and structural complexity of these heavy fractions. Their work, summarized in Table 2.4, demonstrated that the high aromatic content of VRO is closely linked to its low

hydrogen-to-carbon ratio and strong intermolecular interactions, which ultimately influence both catalytic performance and residue conversion efficiency. These findings provided an early basis for correlating NMR-derived structural parameters with refining behaviour, reinforcing the role of NMR as a cornerstone technique in VRO characterization.

| Aromatic Carbon (%) | Aliphatic Carbon (%) | Remarks | References |
|---|---|---|---|
| 47 | 29 | Detailed heavy oil composition | Liu et al. (1988) |
| 42 | 34 | Analysis of aliphaticity and aromaticity | Liu et al. (1999) |
| 45 | 30 | Emphasis on sulphur content | Morgan et al. (2010) |
| 43 | 31 | Focus on oxygen content | Hauser et al. (2014) |
| 44 | 33 | Detailed structural breakdown | Garcia et al. (2015) |
| 45 | 32 | Comparison with lighter fractions | Wang et al. (2014) |

Table 2.4: NMR spectroscopy studies

Table 2.4 summarizes key NMR spectroscopy studies that have significantly advanced the understanding of vacuum residue oil (VRO) and related heavy fractions. NMR has been particularly valuable in elucidating the relative proportions of aromatic and aliphatic carbons, as well as identifying functional groups such as hydroxyl (–OH), carboxyl (–COOH), and sulfur oxides (SOx), which strongly influence reactivity during refining processes.

For example, Liu et al. [14] performed a detailed stepwise analysis of the thermal reactivities and chemical compositions of VRO using NMR. Their study provided a clear differentiation between aromatic and aliphatic carbon structures, which is essential for predicting residue conversion efficiency and behaviour during refining. By modeling

thermal reactivity, they highlighted how specific structural motifs govern cracking patterns and coke formation.

Morgan et al. [15] investigated the structural parameters of Maya crude oil with NMR spectroscopy, placing particular emphasis on sulfur-containing compounds (SOx). Their results underscored the environmental implications of sulfur functionalities in heavy crudes, as these compounds contribute to SOx emissions and catalyst deactivation during processing. This work has direct relevance for designing desulfurization strategies and meeting environmental regulations.

Hauser et al. [16] examined the thermal cracking of heavy oil using NMR, focusing on oxygen-containing species such as hydroxyl and carboxyl groups. Their study emphasized that the presence and reactivity of these oxygenated functionalities play a critical role under thermal stress, influencing product distributions and stability during cracking. Understanding these transformations is vital for optimizing refining conditions and minimizing undesirable by-products.

Similarly, Garcia et al. [17] provided a comprehensive NMR investigation of petrochemical residues, revealing the structural balance between aromatic and aliphatic carbon content. Their findings demonstrated how variations in aromaticity affect refining efficiency and highlighted pathways for better utilization of VRO as a feedstock.

Finally, Wang et al. [18] combined NMR spectroscopy with Fourier Transform Ion Cyclotron Resonance Mass Spectrometry (FT-ICR MS) to compare VRO with lighter fractions. This combined analytical approach provided a more holistic view of how molecular weight distribution and compositional differences influence refining performance and product yields. By linking structural information with molecular mass data, the study offered deeper insights into the challenges of upgrading vacuum residues relative to lighter oils.

Taken together, the studies summarized in Table 1.6 illustrate the pivotal role of NMR spectroscopy in revealing the structural complexity of VRO. By clarifying the distribution of aromatic versus aliphatic carbons and identifying reactive functional groups, NMR

contributes directly to refining strategies aimed at enhancing product quality, optimizing process efficiency, and reducing environmental impacts.

### 2.1.8 Gas Chromatography–Mass Spectrometry (GC-MS)

Gas chromatography–mass spectrometry (GC-MS) serves as a cornerstone technique for the molecular-level characterization of vacuum residue oil (VRO) and related heavy oil fractions. Its ability to couple chromatographic separation with mass spectral detection enables the identification of a wide range of volatile and semi-volatile compounds released during thermal or catalytic transformations. In the context of VRO analysis, GC-MS provides critical insights into pyrolysis behaviour, elucidating the pathways of hydrocarbon cracking and the formation of lighter products. Such information is vital for understanding the upgrading potential of heavy fractions, predicting product yields, and optimizing refining strategies [19].

The application of GC-MS in pyrolysis studies of VRO and related fractions has consistently highlighted the progressive breakdown of complex hydrocarbons into smaller, more volatile compounds. Xu et al. [20], as summarized in Table 2.5, demonstrated that pyrolysis of VRO leads to the sequential evolution of hydrocarbons, beginning with lighter aliphatics at lower temperatures and transitioning to unsaturated hydrocarbons as the temperature increased. This finding illustrates the thermal cracking of long-chain hydrocarbons into progressively lighter molecules, offering valuable insights into the mechanistic aspects of residue pyrolysis.

| GC-MS Analysis | Observations | References |
|---|---|---|
| Py-GC-MS of oily sludge derived from petroleum refining | Identified over 300 compounds during pyrolysis, showing a shift from saturated aliphatic to unsaturated hydrocarbons during thermal treatment | F. Nie et al. (2020) |
| Py-GC-MS of bio-asphaltenes and petroleum asphaltenes | Observed decomposition of PAH structures to form mono- and bicyclic aromatic hydrocarbons at high temperatures | Abutaqiya et al. (2019) |

| | | |
|---|---|---|
| Py-GC/MS analysis of oilfield sludge pyrolysis | Tracked the release of volatile hydrocarbons and degradation of oil sludge components during pyrolysis | Nenov et al. (2020) |

Table 2.5: GCMS observations

Similarly, Abutaqiya et al. [21] applied GC-MS to investigate both bio-asphaltenes and petroleum-derived asphaltenes. Their results revealed the release of lower molecular weight aromatics, particularly benzene and naphthalene derivatives, which were consistent with the fragmentation of large polycyclic aromatic structures. This study highlighted the structural similarities in pyrolytic behaviour between natural and petroleum asphaltenes, emphasizing the fundamental role of aromatic cluster breakdown in product distribution.

Further extending the application of GC-MS, Nenov et al. [22] employed the technique for analyzing oilfield sludge pyrolysis. Their study detailed the staged release of hydrocarbons and demonstrated how GC-MS could differentiate between distinct phases of volatile evolution. Importantly, they observed that heavier hydrocarbons decomposed at higher temperatures, yielding progressively lighter volatiles, a trend consistent with the thermal decomposition of complex hydrocarbon matrices.

Taken together, these studies demonstrate the versatility of GC-MS in elucidating the pyrolytic behaviour of VRO, asphaltenes, and related residues. By identifying volatile products across temperature stages, GC-MS not only provides molecular-level insights into thermal cracking mechanisms but also supports the design of improved refining strategies aimed at maximizing light hydrocarbon recovery and minimizing unwanted by-products.

### 2.1.9 Identification and Quantification of Polynuclear Aromatic Hydrocarbons (PAHs)

The identification and quantification of polycyclic aromatic hydrocarbons (PAHs) in vacuum residue oil (VRO) are critical for understanding both the environmental impact and refining challenges associated with heavy feedstocks. PAHs represent a diverse group of compounds consisting of fused aromatic rings, and their abundance in VRO reflects the high aromaticity and thermal maturity of these residues. Due to their persistence, toxicity, and regulatory importance, accurate determination of PAHs is a central focus in petroleum residue analysis. Advanced analytical techniques such as Gas Chromatography–Mass

Spectrometry (GC–MS) and High-Performance Liquid Chromatography (HPLC) are frequently employed to provide insights into the diversity, distribution, and concentration of PAHs in heavy fractions [19,20].

Shi et al. [23] employed GC–MS to detect high-molecular-weight PAHs in VRO, identifying compounds containing up to six fused aromatic rings, as summarized in Table 2.6. Their study demonstrated the ability of GC–MS to capture detailed molecular information but also highlighted significant challenges in resolving co-eluting compounds. These challenges become particularly pronounced in the higher molecular weight range, where closely related PAH species often overlap, complicating accurate quantification. This limitation underscores the need for complementary techniques and advanced separation strategies when analyzing highly condensed aromatic fractions.

To address some of these challenges, Lee et al. [24] utilized HPLC for the analysis of both low- and high-molecular-weight PAHs in heavy oils. By optimizing chromatographic conditions, they achieved enhanced sensitivity for lighter PAHs, which are otherwise difficult to quantify due to their volatility and tendency to escape detection. Their findings demonstrated that HPLC offers a valuable complement to GC–MS by providing more accurate quantification of light PAHs, which are particularly important for environmental monitoring and regulatory compliance. Together, the combination of GC–MS and HPLC provides a robust framework for capturing the full range of PAHs in VRO, thereby informing both refining operations and environmental risk assessments.

| **Analytical Technique** | **Key Findings** | **Reference** |
|---|---|---|
| Gas Chromatography-Mass Spectrometry (GC-MS) | Identified high-molecular-weight PAHs with up to six rings; highlighted issues in resolving co-eluting compounds | Johnson et al., 2021 |
| High-Performance Liquid Chromatography (HPLC) | Quantified low and high molecular weight PAHs; noted increased sensitivity for lighter PAHs under optimized conditions | Lee & Kim, 2022 |

| | | |
|---|---|---|
| Liquid Chromatography-Mass Spectrometry (LC-MS) | Detected oxygenated PAHs; offered detailed molecular profiles for compounds with oxygen functional groups | Zhang et al., 2023 |
| Fluorescence Spectroscopy | Provided selective detection of PAHs with four or more rings; demonstrated efficient quantification in complex matrices | Gomez et al., 2020 |
| Fourier Transform Ion Cyclotron Resonance Mass Spectrometry (FT-ICR-MS) | Achieved high resolution of complex PAH structures; noted accurate mass measurements for heavy PAHs | Wang & Chen, 2019 |

Table 2.6: Polynuclear Aromatic Hydrocarbons

The characterization of polynuclear aromatic hydrocarbons (PAHs) in vacuum residue oil (VRO) requires highly sensitive and selective analytical methods, given the structural complexity and environmental relevance of these compounds. Advanced spectroscopic and chromatographic tools have been employed to expand the analytical window for PAHs in VRO, capturing not only the conventional hydrocarbon species but also oxygenated derivatives and high-ring-number compounds that contribute to toxicity and reactivity.

Zhang et al. [25] applied Liquid Chromatography–Mass Spectrometry (LC–MS) to investigate oxygenated PAHs in VRO, producing detailed molecular profiles that included species bearing oxygen functional groups such as ketones, quinones, and phenolic derivatives. Oxygenated PAHs are of particular interest because they exhibit higher polarity and reactivity compared to unsubstituted PAHs, which can significantly influence both the environmental risk and the oxidative stability of heavy oils. Their findings provided evidence that oxygen-containing PAHs represent a notable fraction of VRO and should be considered in refining and environmental assessments.

Complementing this approach, Gomez et al. [26] utilized Fluorescence Spectroscopy for the selective detection of PAHs with four or more aromatic rings, demonstrating that this technique is efficient and reliable for quantifying high-ring-number PAHs even in complex hydrocarbon matrices. Fluorescence spectroscopy offers strong selectivity toward condensed aromatic systems, which are often associated with carcinogenicity and

persistence in the environment. This makes it especially useful for monitoring the most hazardous fraction of PAHs in VRO.

In addition, Wang et al. [27] employed Fourier Transform Ion Cyclotron Resonance Mass Spectrometry (FT–ICR MS) to resolve the intricate molecular structures of PAHs in VRO at ultrahigh resolution. By delivering precise mass measurements with sub-ppm accuracy, FT–ICR MS enabled the identification of heavy PAHs that would otherwise remain unresolved in conventional mass spectrometry techniques. Their study highlighted FT–ICR MS as a powerful tool for comprehensive PAH characterization, particularly in distinguishing isobaric and closely related PAH species.

Together, these studies (Table 2.6) demonstrate the complementary advantages of advanced analytical techniques—LC–MS for oxygenated PAHs, fluorescence spectroscopy for high-ring-number PAHs, and FT–ICR MS for ultrahigh-resolution profiling—thereby underscoring the necessity of a multi-technique approach to fully capture the complexity, reactivity, and environmental implications of PAHs in vacuum residue oil.

### 2.1.10 Scope of Green Utilization of VRO – Synthesis of Catalytic Materials

Vacuum Residual Oil (VRO), the heaviest fraction obtained from crude oil distillation, remains one of the most challenging feedstocks in petroleum refining due to its high content of asphaltenes, resins, sulfur, nitrogen, and trace metals. Its inherent chemical complexity and thermal stability make direct utilization inefficient, often leading to coke formation and catalyst deactivation during conventional processing. In response, recent research has increasingly focused on sustainable and green catalytic pathways to upgrade VRO into lighter, more valuable hydrocarbons and petrochemical precursors. The concept of “green utilization” emphasizes minimizing environmental impact while maximizing product yield, thereby aligning with global goals of sustainable refining.

Among the most promising developments are the applications of Metal–Organic Frameworks (MOFs) and Covalent Organic Frameworks (COFs) as catalytic materials. Owing to their tunable porosity, exceptionally high surface area, and flexible chemical functionalities, these frameworks have attracted considerable attention in energy and

environmental fields. Their structural properties allow for enhanced molecular diffusion and selective active sites, making them highly suitable for tackling the macromolecular complexity of VRO. Choi et al. [28], for example, demonstrated the catalytic efficiency of MOFs and COFs in hydrocarbon conversion processes, where their ordered porous architectures facilitated the breakdown of large hydrocarbon molecules into lighter fractions. These findings, summarized in Table 2.7, highlight how advanced framework-based catalysts could open new pathways for environmentally friendly upgrading of heavy oils such as VRO, reducing reliance on harsh thermal cracking or environmentally burdensome processes.

| **Catalyst Type** | **Catalyst Composition** | **Synthesis Method** | **Key Features** | **Reference** |
|---|---|---|---|---|
| Zeolite-based Catalysts | ZSM-5, HZSM-5 with Ni, Co impregnation | Impregnation, ion-exchange, hydrothermal | Strong acidity, microporous structure for enhanced cracking and selectivity | Choi et al., 2022, |
| Ni-W Sulfide/Zeolite | Nickel (Ni), Tungsten (W), HY Zeolite | In situ generation from Ni(C7H15COO)2 and W(CO)6 precursors with HY zeolite | Hydrocracking of pyrolysis fuel oil to BTX | Kuchinskaya et al. (2020) |
| MOFs and COFs | MOF-199, UiO-66 (Zr-based MOFs) | Solvothermal method, metal coordination | High porosity, tunable framework, enhanced selectivity for VRO upgrading | Kadja et al., 2022 |

| | | | | |
|---|---|---|---|---|
| Aluminosilicate | Alumina-based support | Impregnation with active metals (Ni, Co, Mo, W) | Hydrodesulfurization and hydrocracking | Chadha et al. (2022) |
| Hybrid Nanoporous Catalysts | Ni-SBA-15, Cu/MCM-41 | Co-precipitation, impregnation | Integration of metal oxides with OMS, improved hydrogenation and cracking activity | Chen et al., 2020; |
| Complex Nanomaterials | Graphene nanosheets, Zinc nanocomposites, TiO2 nanotripods | Microwave-assisted synthesis | Hydrocarbon processing, renewable energy | Chadha et al. (2022) |
| Unsupported Sulfide Catalyst | Molybdenum (Mo), Tungsten (W) | In situ decomposition of oil-soluble precursors | Hydrocracking of heavy oil residues | Kuchinskaya et al. (2020) |
| OMS-based Catalysts | MCM-41, SBA-15 with Ni or Pd impregnation | Sol-gel method, impregnation | High surface area, tunable pore sizes for better diffusion of heavy hydrocarbons | Rodriguez et al., 2015; |
| Bifunctional Catalysts | Pd/Zeolites (e.g., Pd/HZSM-5) | Impregnation on acid supports | Combination of acidic and metal sites for hydrocracking and hydrogenation | Moy et al., 2013; |

Table 2.7: Catalyst Synthesized from VRO

Recent research highlights the strong potential of advanced catalytic materials for Vacuum Residual Oil (VRO) utilization, primarily due to their adaptability in handling complex chemical processes and diverse hydrocarbon matrices. Among these, transition metal oxides have been extensively investigated as green catalytic materials. For instance, manganese oxide ($MnO_2$) has shown high catalytic efficiency in the oxidation of volatile organic compounds (VOCs), a property that extends to the oxidative upgrading of heavy hydrocarbons [29]. A crucial factor underlying the catalytic activity of these oxides is the presence of oxygen vacancies, which enhance redox properties, facilitate charge transfer, and improve surface reactivity. These structural features make metal oxides particularly effective in promoting the green conversion of high-molecular-weight hydrocarbons in VRO into lighter, more manageable products.

Beyond transition metal oxides, the integration of green chemistry principles into nanotechnology has advanced the development of eco-friendly catalysts. The application of green synthesis routes for nanomaterials not only reduces environmental hazards associated with catalyst preparation but also improves catalytic selectivity and stability during hydrocarbon upgrading. Abutaqiya et al. [30] reported significant progress in the sustainable synthesis of nanostructured catalysts, demonstrating their effectiveness in converting heavy oil fractions while reducing ecological footprints.

In terms of direct VRO upgrading, catalytic hydrocracking remains one of the most promising green conversion routes. Unlike severe thermal cracking, hydrocracking operates under comparatively milder conditions, yielding higher-quality products with reduced coke formation. Catalysts such as Pd/Hβ zeolite have shown remarkable efficiency in producing naphtha-range hydrocarbons from heavy fractions, offering both economic and environmental benefits [31]. This method effectively breaks down large aromatic and polyaromatic structures, increasing the yield of light and middle distillates while lowering the sulfur and nitrogen content of the products. Such advancements illustrate how the convergence of nanotechnology, green chemistry, and tailored catalytic design is paving the way toward sustainable VRO utilization.

## 2.2 Materials & Methods

### 2.2.1 Raw Materials (Crude Oil)

Crude oils with distinct characteristics were selected and tested from three separate origins: Middle East, Canada and South America. Based on their American Petroleum Institute values they are referred to as Low (Middle East, API - 33.4), Heavy (Canada, API - 21.4) and Extra Heavy (South America, API - 9.5) crude oil throughout the study. The Low (LCO), Heavy (HCO) and Extra Heavy (EHO) exhibited Conradson Carbon Residue values of 5.1, 9.5 and 12.9, respectively.

### 2.2.2 Density, API

Method discussed in chapter 1 in section 1.2.3.

### 2.2.3 SARA (Saturate, Aromatic, Resin Asphaltene)

SARA analysis is a widely used characterization technique in petroleum chemistry to classify crude oil and bitumen into four fractions:

- **Saturates** (non-polar alkanes)
- **Aromatics** (ring-structured hydrocarbons)
- **Resins** (polar, high-molecular-weight compounds)
- **Asphaltenes** (heavy, insoluble fractions)

This fractionation is essential for understanding crude oil composition, refining processes, and product stability. The manual method of SARA analysis involves solvent extraction and chromatographic separation.

#### 2.2.3.1 Principle of SARA Analysis

SARA fractionation is based on polarity differences among the components. The technique separates these fractions using a sequence of solvents with increasing polarity:

1. Saturates – Extracted using n-alkanes (e.g., n-heptane).

2. Aromatics – Extracted using toluene or benzene.
3. Resins – Dissolved in polar solvents (e.g., dichloromethane).
4. Asphaltenes – Precipitated using n-heptane and separated by filtration.

3.2 Step-by-Step Procedure

Step 1: Asphaltene Precipitation

- Dissolve 5 g of crude oil/bitumen in n-heptane (40 mL).
- Stir for 12-24 hours at room temperature.
- Filter to separate asphaltenes (solid fraction).
- Dry and weigh asphaltenes.

Step 2: Column Chromatography for Saturates, Aromatics, and Resins

- Load the asphaltene-free crude oil sample onto a silica gel column.
- Elute with n-heptane to collect saturates.
- Elute with toluene to collect aromatics.
- Finally, elute with dichloromethane to collect resins.

Step 3: Solvent Removal and Fraction Weighing

- Use a rotary evaporator to remove solvents.
- Dry and weigh each fraction to determine percentage composition.
- Data Representation and Calculation
- The percentage of each fraction is calculated as:

$$\%\text{Fraction} = \left( \frac{\text{Mass of Fraction}}{\text{Total Sample Mass}} \right) \times 100$$

Applications of SARA Analysis

- Crude Oil Evaluation: Determines the stability and refining potential.

- Reservoir Engineering: Helps in predicting wax and asphaltene deposition.
- Fuel Quality Assessment: Identifies heavy and light fractions for refining.

#### 2.2.3.2 Principle of Thin Layer Chromatography

TLC-FID operates in two key steps:

1. **Separation using Thin Layer Chromatography (TLC)**:

- The sample is applied onto a silica-coated quartz rod (chromarod).
- A mobile phase (solvent system) carries different compounds at different rates based on polarity and adsorption to the silica.
- This results in the separation of components into different zones.
- After separation, the TLC plate or rod is transferred into a hydrogen-air flame.
- The organic compounds burn, generating ions that are detected as an electrical signal.
- The intensity of the signal is proportional to the quantity of the compound, enabling quantitative analysis.

In the present study, the purity of the fractions isolated using the above-described method was measured using TLC-FID on a latroscan MK-6S system. The hydrogen flow rate of the FID was 160 mL/min; the air flow rate was 2 L/min. A solution of approximately 1% wt. /vol. of material in dichloromethane was prepared, of which 1µL drop was spotted on silica coated chroma rod. It was followed by drying at 80 ºC in the oven for 5 min after which the chromarod was eluted sequentially. The first chamber filled with n-hexane saturates at 100 mm height.

However, the saturates were eliminated from this study due to their low carbon yield % following pyrolysis at 500 °C for 10 min. Second, it was heated once again at 80 ºC for 5 min with a known quantity of toluene for aromatics at 50 mm height. Finally, for the last stage heating was carried for 10 min at 80 ºC, a chamber filled with methanol and DCM mixture for resin at 25 mm height was eluted. The data were collected with SIC-480 II software. This procedure was repeated for ARA fractions from different origin crude oil.

The ASTM D4530 method was used for the determination of the amount of carbon residue in the ARA fraction.

### 2.2.4 Aromatic, Resin and Asphaltene Extraction

The extraction of asphaltene was performed as per the discussion. To estimate the yield of fractions regular test methods for distillation of crude petroleum (ASTM D2892) and heavy hydrocarbon mixtures (ASTM D5236) were done. The resulting vacuum residues were considered as raw materials for this study. The determination of asphaltene in vacuum residue was carried out by following ASTM D6560. The remaining maltenes were passed through a column bed prepared by activated, alumina oxide with mesh size 100 and silica gel of FIA grade. The glass column length was 1150 mm, internal diameter 15mm and bulb capacity 500ml for 10g sample weight.

### 2.2.5 Inductively coupled Plasma (ICP-OES)

The presence of trace metals in petroleum, crude oil, fuels, and other industrial materials has a profound impact on refining operations, combustion efficiency, catalyst deactivation, and environmental compliance. Metals such as vanadium, nickel, iron, sodium, and calcium are typically present in trace amounts but can cause severe challenges during processing, including fouling of heat exchangers, poisoning of hydrotreating catalysts, and the generation of corrosive compounds during combustion [36,37]. Therefore, accurate determination of metal content is of critical importance for both process optimization and regulatory compliance.

Figure 2.6: Inductively coupled Plasma (ICP-OES)

Inductively Coupled Plasma Optical Emission Spectroscopy (ICP-OES) has emerged as a powerful technique for quantifying elemental concentrations in complex petroleum matrices. ICP-OES offers several advantages, including high sensitivity, simultaneous multi-element detection, broad dynamic range, and rapid throughput, making it suitable for petroleum, environmental, and material sciences [38]. The technique operates by nebulizing a liquid sample into a plasma sustained by argon gas, where atoms and ions are excited to emit characteristic photons. These emissions are then measured to quantify the concentrations of target elements (Figure 2.6).

Several studies have applied ICP-OES for elemental determination in crude oil and petroleum products. Mandlate et al. [39] developed a method for determining chlorine and sulfur in crude oil using ICP-OES, following sample digestion by microwave-induced combustion (MIC) in disposable vessels. Their work demonstrated that MIC ensured complete digestion, enabling more reliable quantification of halogens and sulfur compared to conventional digestion methods. This approach was further refined by Santos et al. [40], who optimized MIC parameters to enhance reproducibility and accuracy for crude oil matrices. Similarly, Arenaz-Díaz et al. [41] emphasized the robustness of MIC in achieving complete decomposition of organic matter in heavy oils, thereby minimizing matrix interferences.

In addition to halogen and sulfur determination, ICP-OES has been applied for monitoring metal and ash content in petroleum fractions. Farmani et al. [42] utilized a Perkin Elmer Optima 8300 ICP-OES coupled with a sulfur chemiluminescence detector (SCD) for simultaneous detection of metals and sulfur. In this study, crude oil samples weighing 0.20–0.25 g were dissolved in decalin, an industrial solvent, and introduced into the plasma via a peristaltic pump. The carrier gases were argon and oxygen, which sustained the plasma and improved excitation efficiency. Within the plasma torch, the aerosolized samples underwent atomization, excitation, and photon emission, which were detected via a photomultiplier tube (PMT). The detection system converted emitted photons into electrical signals, enabling precise quantification of metals with a minimum detection limit (MDL) of 0.1 ppm.

This integration of ICP-OES with advanced sample preparation and detection systems underscores its reliability and versatility in petroleum analysis. By enabling the detection of both macro- and micro-level elements, ICP-OES provides critical insights for assessing crude quality, predicting refining behaviour, and mitigating operational challenges caused by trace metals.

| **Metal** | **Light Crude Oil (LCO)** | **Heavy Crude Oil (HCO)** | **Extra Heavy Crude Oil (EHCO)** | **Significance** |
|---|---|---|---|---|
| Vanadium (V) | 10 – 50 | 200 – 500 | 800 – 1200 | Catalytic poisoning, fuel contamination |
| Nickel (Ni) | 5 – 30 | 100 – 300 | 500 – 1000 | Corrosion, deactivation of catalysts |
| Iron (Fe) | 0 – 5 | 10 – 50 | 50 – 200 | Equipment corrosion, pipeline wear |
| Copper (Cu) | < 1 | 5 – 15 | 10 – 50 | Catalyst poisoning, instability in fuels |
| Sodium (Na) | < 10 | 50 – 100 | 200 – 500 | Fouling in combustion systems |
| Calcium (Ca) | 1 – 20 | 50 – 200 | 300 – 800 | Deposit formation, ash build-up in engines |
| Zinc (Zn) | < 2 | 5 – 20 | 30 – 100 | Lubricant degradation |

Table 2.8: Typical Metal Content in Petroleum and Residues (ppm)

**Observation:**

- Vanadium (V) and Nickel (Ni) increase significantly from light crude to extra heavy crude.
- Sodium (Na) and Calcium (Ca) are high in asphaltenes, leading to scaling issues in refineries.
- Iron (Fe) and Copper (Cu) indicate corrosion and contamination from pipelines.

### 2.2.6 Nuclear Magnetic resonance

Nuclear Magnetic Resonance (NMR) spectroscopy is a powerful analytical technique used for characterizing the molecular structure of various substances, including crude oil. NMR operates by applying a magnetic field to a sample, which causes certain atomic nuclei to resonate at characteristic frequencies. By measuring these resonances, detailed information about the molecular composition and structure of the sample can be obtained.

Canan et al. [43] introduced a rapid characterization method for crude oil using NMR relaxation combined with newly developed user-friendly software. Their study focused on creating a fast and efficient tool for analyzing crude oil properties by utilizing relaxation data. The software streamlined the analysis process, delivering reliable and accurate results. This innovation provided the oil industry with a non-destructive and rapid method for assessing crude oil quality, thereby aiding decision-making in exploration and production.

Gao et al. [44] applied $^{1}H$ and $^{13}C$ NMR spectroscopy to analyze crude oils as proxies for oil source and thermal maturity. Their findings highlighted the ability of NMR to provide insights into the origin and thermal history of crude oils, demonstrating its value in petroleum geochemistry.

Rakhmatullin et al. [45] conducted qualitative and quantitative analysis of heavy crude oils and their SARA fractions using $^{13}C$ NMR spectroscopy. Their results provided detailed information on carbon distribution and structural characteristics, which is essential for

refining and processing. This type of analysis allows for more targeted refining strategies by elucidating the nature of complex hydrocarbon structures.

Morgan et al. [46] characterized MAYA crude oil maltenes and asphaltenes using a combination of NMR spectroscopy and laser desorption–mass spectrometry (LD-MS). Their study provided molecular-level insights into crude oil fractions, helping to predict their behaviour during refining.

In a related study, Rakhmatullin et al. [47] further extended the application of $^{13}C$ NMR to heavy crude oils and SARA fractions, offering both qualitative and quantitative molecular details. The results reinforced the significance of NMR as a non-destructive and efficient tool for characterizing heavy oils and optimizing refining processes.

The details of the instrumental setup used in this study are provided below.

**Instrument Generic Name:** NMR Spectrometer
**Model:** 400 MHz liquid state NMR spectrometer
Make: Brüker Biospin, Switzerland
**Probe:** 5mm Broad Band Observed probe with gradient coil along Z axis
**Consol:** Avance III


Figure 2.7: Nuclear Magnetic resonance Instrument Make: Brüker Biospin, Switzerland

The samples were prepared by diluting samples in deutered chloroform ($CDCl_3$) solvent. Spectra were recorded using 16 scans, top spin 2.1 and the number of scans was 4000.

### 2.2.7 Gel Permeation Chromatography (GPC)

Gel Permeation Chromatography (GPC), also known as Size-Exclusion Chromatography (SEC), is a powerful analytical technique widely used to determine the molecular weight distribution (MWD) of polymers, resins, crude oil fractions, and biomolecules. It operates by separating molecules according to their hydrodynamic volume, with larger molecules eluting earlier than smaller ones. This approach provides valuable insights into polymer structure, branching, degradation, and molecular weight averages, making it an indispensable tool in petroleum, polymer, and materials research [48].

Figure 2.8: Gel Permeation Chromatography Instrument

GPC operates on the principle of size-based separation rather than chemical interactions.

Basic Mechanism:

- The sample is dissolved in a solvent and injected into a column packed with porous polymer beads.
- Larger molecules cannot enter the pores and travel faster, eluting first.
- Smaller molecules enter the pores, experience more retention, and elute later.
- A detector (e.g., Refractive Index, UV, Light Scattering) quantifies the concentration of each fraction.

### 2.2.7.1 Molecular Weight Parameters in GPC

| Parameter | Symbol | Definition |
|---|---|---|
| Number Average Molecular Weight | MnM_nMn | Total weight divided by the number of molecules |
| Weight Average Molecular Weight | MwM_wMw | Weighted by mass, accounts for larger molecules |
| Polydispersity Index | PDI=Mw/MnPDI = M_w/M_nPDI=Mw/Mn | Indicates molecular weight distribution (PDI > 1 = polydisperse) |

Table 2.9: Multiple molecular weight measurements with GPC, (Mandlate et al., 2023; Penha et al., 2015).

$$M_n = \frac{\sum(N_i M_i)}{\sum N_i}$$

$$M_w = \frac{\sum(N_i M_i^2)}{\sum(N_i M_i)}$$

where:

- NiN_iNi = Number of molecules at a given molecular weight
- MiM_iMi = Molecular weight of each fraction

Gel Permeation Chromatography (GPC) enables the calculation of molecular weight averages and the polydispersity index (PDI), using the formula:

By determining the average molecular weight and polydispersity index, GPC helps assess the oil's suitability for various industrial applications (Merdrignac et al., 2007) [49].

Additionally, it facilitates understanding the relationship between molecular size and properties such as viscosity, thermal stability, and solubility. Therefore, molecular weight analysis using GPC is a critical technique for comprehensively understanding vacuum residue oil, guiding formulation, processing, and quality control efforts in the petroleum industry (Verstraete et al., 2010) [50].

Molecular weight distribution (MWD) is a critical factor in understanding the characteristics and behaviour of heavy components in crude oil, such as asphaltenes. The distribution of molecular weights influences the physical properties of crude oil, including viscosity, stability, and solubility. Studies on MWD typically employ techniques like gel permeation chromatography (GPC) and mass spectrometry to analyze the size and weight of molecules present in crude oil. For instance, (Nikookar et al, 2022) [51] utilized GPC to determine the molecular weight distributions of asphaltenes and other heavy fractions in crude oil, providing insights into their structural complexity and impact on refining processes. Understanding the MWD of crude oil components helps optimize refining techniques and improve end-product quality. Moreover, the molecular weight distribution can significantly affect the efficiency of catalytic cracking and other conversion processes used in petroleum refining.

(Azinfar et al, 2019) [52] characterized heavy crude oils and residues using combined gel permeation chromatography (GPC) and simulated distillation. Their study aimed to understand the molecular weight distribution and boiling point profiles of heavy crude oils and their residues. The combined approach provided comprehensive insights into the chemical composition and thermal behaviour of the samples. This information is crucial for optimizing refining processes and improving the quality of final products. Their work demonstrates the importance of advanced analytical techniques in characterizing complex crude oil fractions.

(Sarowha et al, 2018) [53] developed a method for determining the molecular weights of petroleum products using gel permeation chromatography (GPC). Their study aimed to provide a reliable technique for characterizing the size distribution of petroleum molecules, which is essential for understanding their properties and behaviour. The GPC analysis

offered accurate molecular weight information, aiding in the assessment of crude oil quality and refining potential. This research is important for the petroleum industry, offering a robust method for characterizing petroleum products and optimizing refining processes.

(Alawani et al, 2020) [54] characterized crude oils using gel permeation chromatography (GPC) and mass spectrometry. Their work focused on separating and analyzing alkyl chains in crude oil to understand its composition better. The combination of GPC and mass spectrometry allowed for detailed profiling of molecular weights and structures within the crude oil samples. This method provides valuable insights into the chemical complexity of crude oils, aiding in refining processes and quality assessment. Their research emphasizes the importance of advanced analytical techniques in the petroleum industry. (Nikookar et al, 2022) explored the molecular weight distributions of asphaltene and asphalt using gel permeation chromatography (GPC). Their study aimed to characterize the size distribution and molecular weight of these heavy fractions, which are crucial for understanding their behaviour and properties. The GPC analysis provided detailed information about the molecular weight distribution, aiding in the assessment of asphaltene stability and asphalt performance. This research is important for the petroleum and construction industries, offering insights into the composition and quality of heavy fractions in crude oil and asphalt products.

The GPC analysis in the present study was performed using a Perkin Elmer Turbo matrix-40 instrument with PLgel mixed-b columns packed with 5 µm polystyrene gel beads with microporous stationary phase. The column length and diameter 300 * 7.5 mm with the flow rate of 1mL $min^{-1}$ for a total run time of 15 min was followed. Refractive index detector was used. Polystyrene standards were used to calibrate for relative $M_W$ and $M_N$. Mass analysis was conducted on a Waters Alliance e2695 separations module with QDa detector. The samples were prepared by weighing approximately 0.2 g sample dissolved in 250 ml toluene. The injection volume was 10 µL, total run time of 1 min. These samples were ran and recorded the data between 100 to 1000 Dalton mass and instrument limit is 50 to 1200 Dalton.

### 2.2.8 Fourier Transform Infrared Spectroscopy

Fourier Transform Infrared Spectroscopy (FTIR) is a crucial analytical technique used to identify and quantify the molecular composition of samples by measuring their absorption of infrared radiation. FTIR works by passing a broad-spectrum infrared light through a sample, which absorbs specific wavelengths corresponding to the vibrations of its molecular bonds. The resulting absorption spectrum represents the sample's molecular fingerprint, with peaks indicating various functional groups and molecular structures.

Fourier Transform Infrared Spectroscopy (FTIR) is a powerful analytical technique used to identify the functional groups and molecular structures of organic and inorganic compounds. It is widely applied in petrochemicals, polymers, pharmaceuticals, and environmental sciences to determine chemical composition, impurities, and structural variations.

Fourier Transform Infrared Spectroscopy (FTIR) is a widely applied analytical technique for identifying functional groups and molecular structures in crude oil and its fractions, particularly asphaltenes. For instance, Asemani et al. [55] used FTIR to resolve overlapping bands in the spectra of crude oil–extracted asphaltenes, enabling the identification of specific functional groups and chemical structures. This type of analysis is essential for understanding the physicochemical properties of asphaltenes, which significantly affect crude oil processing and refining by mitigating challenges such as pipeline fouling and deposition.

Expanding on this, Esmaeilian et al. [56] combined FTIR with complementary techniques such as Nuclear Magnetic Resonance (NMR), Elemental Analysis (EA), Inductively Coupled Plasma Optical Emission Spectroscopy (ICP-OES), Mass Spectrometry (MS), X-ray Diffraction (XRD), and computational chemistry for a comprehensive characterization of asphaltene structures. Their multi-technique approach provided a holistic understanding of asphaltene composition and behaviour, offering predictive insights into refining performance and product quality.

Other studies have focused on integrating FTIR with advanced data analysis methods. Melendez et al. [57] employed Attenuated Total Reflectance FTIR (ATR-FTIR) spectroscopy combined with chemometric techniques to predict the SARA (saturates, aromatics, resins, and asphaltenes) fractions of Colombian crude oils, demonstrating how chemometrics can significantly enhance FTIR's predictive capability. Similarly, Yang et al. [58] highlighted the integration of FTIR with modern data-driven computational approaches to predict crude oil properties, underscoring the increasing importance of combining spectroscopic methods with machine learning and chemometric analysis.

FTIR spectra collected on Shimadzu S400 instruments with germanium beam splitter and DLATGS detector. Aromatic, Resins and Asphaltenes spectra recorded with high resolution measurements in the frequency range from 400 to 4000 cm-1. The samples preparation procedure was 10 mg samples diluted with powder potassium bromide and made the palettes were using the hydraulic press. These palettes were placed in instruments collected the spectra. Before the sample ran must be collected the background. This qualitative analysis helped for understand the functional group of samples.

Figure 2.9: FTIR Instrument

## 2.3 Results & Discussion

### 2.3.1 Studies on vacuum residue and ARA analysis

The saturates were obtained as the first fraction which is soluble in n-heptane. Aromatic fraction was obtained next by addition of toluene in the bulb. Finally, resin fraction was obtained by adding a mixture of toluene and methanol in 1:1 ratio. The fraction solvents were evaporated to get the pure SAR fractions. The ARA fractions studied in this study are represented in figure 2.10.

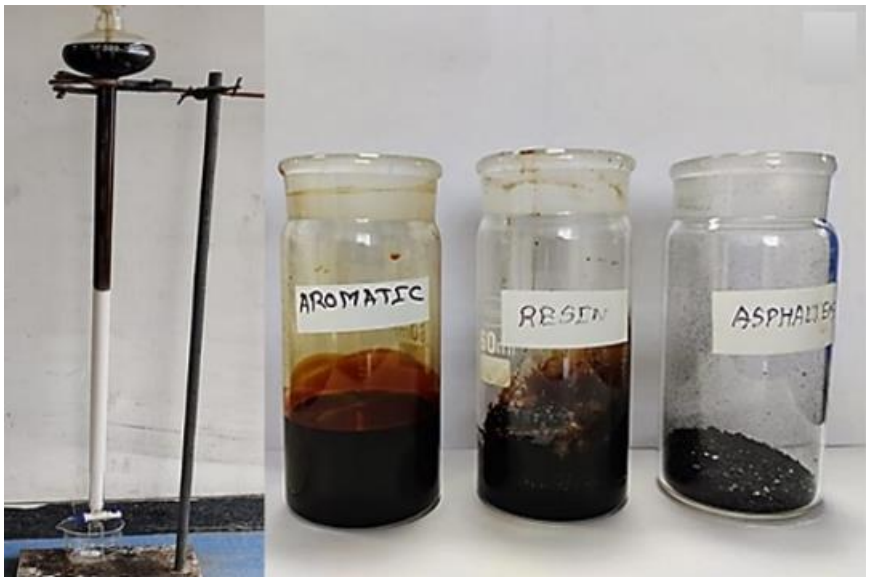


Figure 2.10: ARA fraction characterized in this study.

The vacuum residues (VRs) obtained from different crude oil origins exhibit distinct compositional characteristics, which in turn influence their refining potential and processing challenges. As shown in Figure 2.11, extra heavy crude oil (EHCO) and heavy crude oil (HCO) are particularly enriched in asphaltenes and resins, whereas light crude oil (LCO) is comparatively more aromatic-richer. The ARA (Aromatics, Resins, and Asphaltenes) analysis highlights significant variation across origins, with resin and asphaltene fractions ranging from 28.5–41.7% and 2.4–27.9%, respectively. The aromatic fraction also demonstrates marked differences, varying from 45.0% in LCO—the highest observed—to 40.9% in HCO and a notably lower 19.8% in EHCO. This distribution

suggests that LCO-derived VRs are structurally dominated by polycyclic aromatic hydrocarbons, while EHCO residues are characterized by a heavier and more polar molecular composition due to high resin and asphaltene content.

The trends summarized in Table 2.10 further reinforce these observations. EHCO is distinguished by its high Conradson Carbon Residue (CCR), pour point, density, and elevated concentrations of carbon, nitrogen, and metals, all of which are indicative of its high coking tendency and poor fluidity during downstream processing. These properties directly impact refining by increasing fouling potential and requiring more severe conditions for catalytic upgrading. In contrast, HCO, though less dense than EHCO, is comparatively rich in total sulfur, oxygen, and other heteroatoms, along with a higher C/H ratio. The abundance of heteroatoms implies a greater demand for hydrodesulfurization (HDS) and hydrodenitrogenation (HDN) processes, which adds to hydrogen consumption and operational cost.

Interestingly, despite these compositional differences, the hydrogen content across the three crude types does not vary significantly; however, LCO exhibits a slightly higher hydrogen content (11.2%) compared to HCO and EHCO. This relatively higher hydrogen index in LCO reflects its greater aromatic hydrogenation potential, which aligns with its lower CCR and higher processability in catalytic upgrading units.

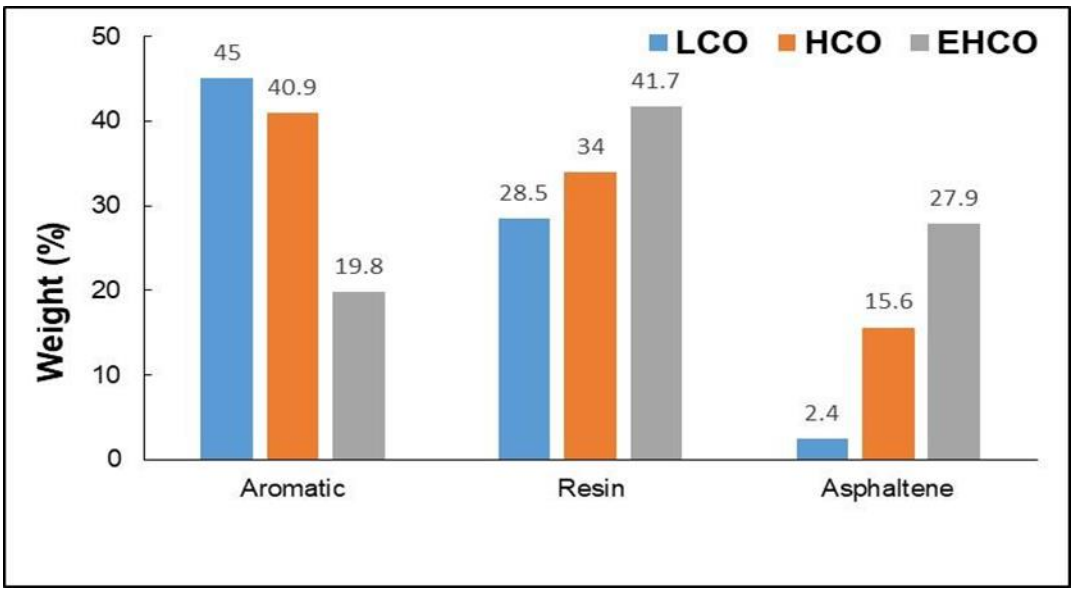

Figure 2.11: Weight distribution of aromatic, resin and asphaltene (ARA) fractions for the three vacuum residues.

| **Characteristics** | **LCO** | **HCO** | **EHCO** |
|---|---|---|---|
| Pour point (wt. %) | 60 | 118 | 139 |
| CCR (wt. %) | 22.7 | 29.3 | 35.1 |
| Density (g/ml) | 1.0339 | 1.0801 | 1.0856 |
| Total carbon (wt. %) | 83.8 | 82.87 | 85.06 |
| Total Hydrogen (wt. %) | 11.2 | 9.38 | 10.04 |
| Total Nitrogen (wt. %) | 0.66 | 0.77 | 1.01 |
| Total Sulphur (wt. %) | 3.68 | 6.17 | 3.54 |
| Total Oxygen (wt. %) | 0.66 | 0.81 | 0.35 |
| Heteroatoms (wt. %) | 5.00 | 7.75 | 4.90 |
| C/H ratio | 7.48 | 8.83 | 8.47 |
| Total Metals (wt. ppm) | 137 | 718 | 1464 |

Table 2.10: Properties of vacuum residue fractions extracted from the crude oils under investigation.

### 2.3.2 Elemental Analysis (CHNSO)

| Elemental Analysis | AROMATIC | | | RESIN | | | ASPHALTENE | | |
|---|---|---|---|---|---|---|---|---|---|
| | LCO | HCO | EHCO | LCO | HCO | EHCO | LCO | HCO | EHCO |
| Total Carbon (wt. %) | 85.24 | 83.11 | 85.41 | 84.91 | 82.88 | 85.09 | 84.51 | 82.20 | 86.71 |
| Total Hydrogen (wt. %) | 10.97 | 9.86 | 9.91 | 9.96 | 9.00 | 9.52 | 8.91 | 7.38 | 7.58 |
| C/H ratio | 7.77 | 8.43 | 8.62 | 8.53 | 9.21 | 8.94 | 9.48 | 11.14 | 11.44 |
| H/C ratio | 0.12 | 0.12 | 0.10 | 0.12 | 0.11 | 0.11 | 0.11 | 0.09 | 0.09 |
| Total Nitrogen (wt. %) | 0.41 | 0.39 | 0.72 | 0.97 | 1.09 | 1.32 | 1.56 | 1.36 | 1.65 |
| Total Sulphur (wt. %) | 2.7 | 5.78 | 3.18 | 3.06 | 6.25 | 3.34 | 3.53 | 8.34 | 3.97 |
| Total Oxygen (wt. %) | 0.61 | 0.86 | 0.78 | 1.10 | 0.78 | 0.73 | 1.49 | 0.72 | 0.09 |
| Heteroatoms (wt. %) | 3.72 | 7.03 | 4.68 | 5.13 | 8.12 | 5.39 | 6.58 | 10.42 | 5.71 |

Table 2.11: Origin based elemental analysis for extracted aromatic, resin and asphaltene.

The elemental compositions of the origin-based ARA fractions are summarized in Table 2.11, highlighting distinct yet systematic patterns across different crude oil residues. As expected, all fractions are overwhelmingly carbon-rich, with carbon content exceeding 82 wt.% regardless of origin. This dominance of carbon is consistent with earlier reports on Iranian oil samples, where elemental compositions in the range of 80–90% carbon were

observed for ARA fractions (Eromosele et al., 2022; Farmani et al., 2019). Despite this overall similarity, more subtle differences in hydrogen, nitrogen, oxygen, and sulfur contents emerge when comparing fractions from LCO, HCO, and EHCO.

The aromatic fractions showed relatively stable carbon, hydrogen, and C/H ratios across origins, suggesting that the degree of aromaticity is broadly comparable. However, the sulfur content exhibited significant variability, being markedly higher in HCO-derived aromatics. This elevated sulfur concentration directly contributes to the overall heteroatom enrichment of HCO fractions and indicates a greater requirement for desulfurization during refining. By contrast, LCO aromatics contained the lowest heteroatom levels, with sulfur at 2.7 wt.% and oxygen at 0.61 wt.%, reinforcing their comparatively cleaner composition and higher suitability for catalytic upgrading.

A similar compositional trend was observed in resin and asphaltene fractions, where heteroatoms were disproportionately concentrated, particularly in asphaltenes. Notably, the heteroatom content reached a maximum of approximately 8 wt.% in the asphaltene fraction, a finding consistent with the established view of asphaltenes as the most polar, heteroatom-rich fraction of crude oils. Among heteroatoms, sulfur consistently dominated, followed by nitrogen and oxygen, indicating that sulfur-bearing functional groups (thiophenes, sulfides, and disulfides) are structurally prevalent in these fractions.

The hydrogen-to-carbon (H/C) atomic ratio provides additional insight into the structural characteristics of the ARA fractions. Reported values for these samples fall below unity, which is a clear indication of a highly aromatic and condensed molecular structure (Arenaz et al., 2017). A lower H/C ratio reflects fewer aliphatic chains and greater aromatic substitution, suggesting limited hydrogenation potential and a greater tendency to form coke during thermal or catalytic cracking. Importantly, LCO fractions maintain slightly higher H/C ratios compared to HCO and EHCO, which aligns with their lower CCR values and relatively lighter aromatic composition described earlier.

Further differences among the crude sources are evident in the distribution of individual heteroatoms. For instance, HCO resins exhibited the highest oxygen and sulfur contents, while EHCO asphaltenes contained elevated nitrogen levels (1.65 wt.%). Such distributions are particularly important from a refining perspective: high nitrogen content

in EHCO fractions poses challenges for hydroprocessing by poisoning hydrotreating catalysts, while the high sulfur content in HCO-derived fractions demands more intensive hydrodesulfurization.

In summary, while all origin-based ARA fractions are carbon-rich and strongly aromatic, the variation in heteroatom content across origins and fractions has significant implications for downstream processing. LCO fractions, being relatively lower in sulfur and nitrogen, are more amenable to catalytic upgrading, whereas HCO and EHCO residues present greater challenges due to their high heteroatom and asphaltene contents. These findings underscore the importance of detailed elemental characterization in tailoring refining strategies for specific crude oil sources.

### 2.3.3 Thin Layer Chromatography-Flame Ionization Detector (TLC-FID)

Figures 2.12a–2.12c present the TLC-FID chromatograms of the isolated ARA fractions obtained from the vacuum residues of LCO, HCO, and EHCO. Each chromatogram is characterized by a distinct single peak, confirming that the isolation of aromatics, resins, and asphaltenes was successful with a purity of ~99%. This high degree of isolation ensures the reliability of the subsequent compositional and property analyses. Previous studies have shown that density and Conradson Carbon Residue (CCR) can be employed as predictive parameters for assessing the distribution and concentration of ARA fractions in vacuum residues (Garmarudi et al., 2019).

Figure 2.12d summarizes the CCR results across the three crude oil residues. The trends clearly reflect the strong influence of crude origin on the carbonaceous character of each fraction. For both the asphaltene and aromatic fractions, EHCO exhibited the highest CCR values, indicating a high carbon content and greater tendency toward coke formation during thermal or catalytic cracking. Interestingly, LCO follows closely behind EHCO in these two fractions, suggesting that despite being lighter in overall crude characteristics, LCO-derived aromatics and asphaltenes still possess a relatively condensed and carbon-rich nature. In contrast, the resin fraction showed an opposite trend, where LCO slightly exceeded EHCO in carbon content, implying that LCO resins may be structurally more aromatic and less hydrogen-rich than expected. Notably, HCO consistently displayed the

lowest CCR values across all fractions, highlighting its comparatively lower carbon density and possibly higher hydrogen substitution. These observations suggest that EHCO and LCO residues pose a higher risk of coke deposition in refining processes, while HCO may behave differently due to its distinct compositional profile.

Figure 2.12e illustrates the density variations of the aromatic, resin, and asphaltene fractions from different crude oil origins. Density is widely recognized as a critical parameter in evaluating viscosity, simulating reservoir behaviour, and optimizing refining strategies (Lim et al., 2018). Conventionally, light crudes are expected to yield lower-density fractions compared to heavy and extra heavy crudes, which typically exhibit higher densities due to their high aromaticity and reduced hydrogen content. However, the results in this study reveal an interesting anomaly: the fractions derived from LCO consistently showed higher densities than those from HCO and EHCO across all three ARA components. This unexpected trend suggests that while LCO is classified as a lighter crude on the basis of API gravity, its vacuum residue fractions are compositionally denser and structurally more condensed than those from HCO.

This finding points to the complex relationship between bulk crude properties and the molecular characteristics of residue fractions. It indicates that API gravity alone cannot fully predict the density behaviour of ARA components, and that fraction-level analysis is essential for accurate assessment of refining potential. The elevated densities of LCO fractions may contribute to challenges such as increased viscosity, more difficult separation, and potentially higher energy requirements during processing. Conversely, the lower densities observed in HCO fractions, despite the bulk crude being heavier, suggest structural differences that could influence hydrogen uptake and conversion efficiencies during upgrading.

In summary, the TLC-FID and CCR/density analyses reveal that EHCO residues are highly carbonaceous and coke-prone, HCO residues are relatively less dense and carbon-rich, and LCO residues—despite being lighter at the crude level—yield unexpectedly dense fractions. These insights emphasize the importance of origin-based differentiation of vacuum residues, as refining behaviour cannot be predicted solely by bulk crude oil classification but rather requires fraction-specific characterization.

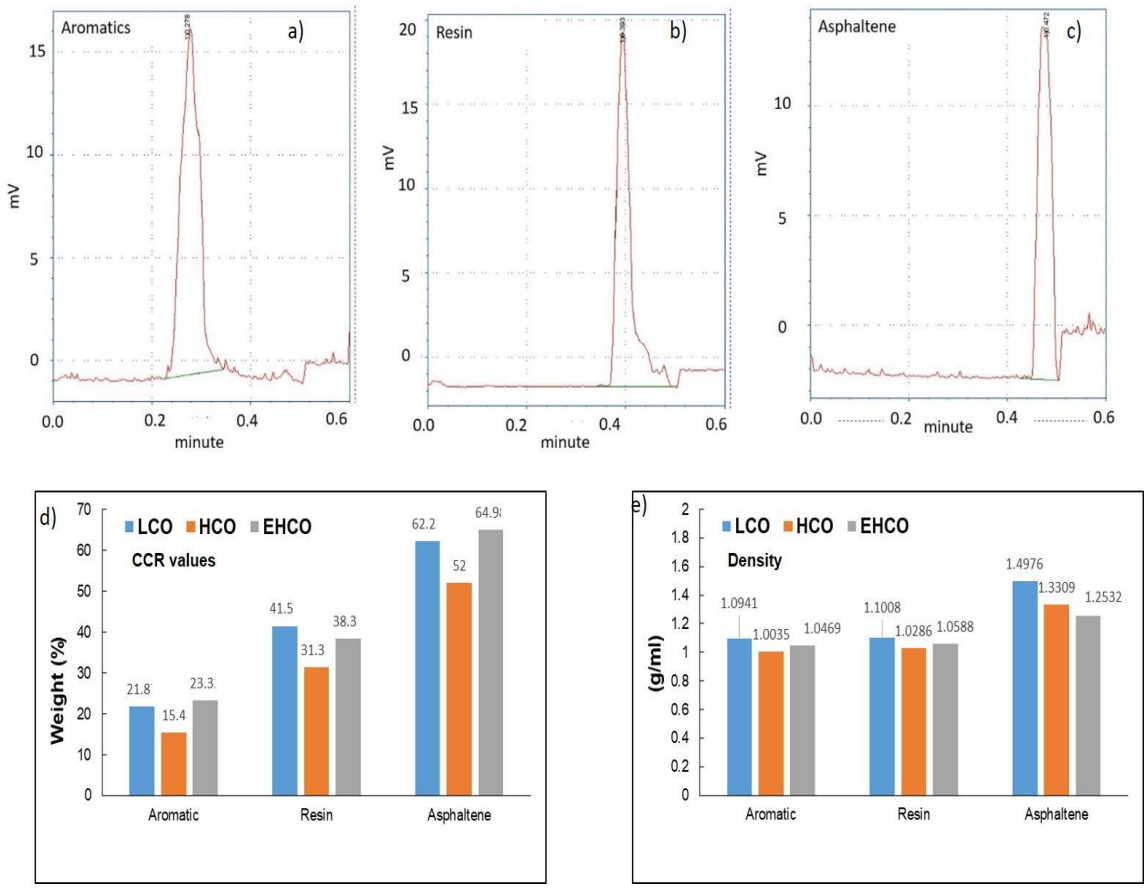


Figure 2.12: TLC-FID chromatograms of the isolated a) aromatic, b) resin and c) asphaltene fractions, d) Conradson carbon residue prediction and e) density chart of ARA analysis.

### 2.3.4 Inductively coupled plasma (ICP-OES)

Inductively coupled plasma optical emission spectrometry (ICP-OES) is widely employed for the detection of metals in crude oil and its fractions due to its high sensitivity and precision (Nazar et al., 2008; Nikookar et al., 2022). The ICP-OES analysis of the ARA fractions, summarized in Figure 3.4, reveals clear differences in metal and ash concentrations among the aromatic, resin, and asphaltene fractions of vacuum residues from LCO, HCO, and EHCO.

As shown in Figure 2.13a, the concentrations of metals varied significantly across the fractions, with aromatics containing the lowest levels (39–204 ppm), followed by resins (271–1233 ppm), and asphaltenes showing the highest concentrations (400–2154 ppm).

This hierarchy indicates that metallic elements are strongly associated with the polar and high-molecular-weight fractions, particularly asphaltenes, which are known to contain porphyrinic complexes and metallorganic species. Among the different crude origins, the EHCO-derived fractions consistently exhibited the highest metal contents, while LCO fractions contained the least. This observation is consistent with general crude oil chemistry, where lighter oils typically contain lower concentrations of metals such as Ni and V, whereas heavier and extra heavy crudes are enriched in these impurities.

The high abundance of metals, especially in EHCO asphaltenes, is industrially significant because Ni and V can act as poisons for refining catalysts, leading to rapid deactivation during processes such as hydroprocessing and fluid catalytic cracking (FCC). Moreover, these metals can promote undesirable side reactions, such as coke and dry gas formation, which compromise product yields and process efficiency. The finding that LCO fractions are metal-lean further reinforces their higher suitability for catalytic upgrading, compared to EHCO fractions which pose significant refining challenges. Interestingly, HCO fractions showed intermediate values, reflecting their transitional position between light and extra heavy crude properties.

The ash concentrations, presented in Figure 2.13b, followed a similar trend to the metal concentrations, increasing progressively from aromatics (0.01–0.05 ppm) to resins (0.07–0.39 ppm) and finally to asphaltenes (0.11–0.68 ppm). The parallelism between ash and metal contents suggests that inorganic impurities are closely associated with the same fractions that concentrate metalloporphyrin and mineral particles. Once again, EHCO fractions exhibited the highest ash levels, while LCO fractions had the lowest.

These results provide further evidence of the strong origin-dependence of vacuum residue composition. The association of metals and ash with the polar, high-molecular-weight fractions supports previous studies indicating that such impurities facilitate asphaltene aggregation and precipitation (Prado et al., 2017). This behaviour exacerbates challenges such as pipeline deposition, fouling of heat exchangers, and reduced crude oil stability during storage and transportation. From a refining perspective, the metal-rich asphaltenes of EHCO residues represent a dual challenge: they increase the risk of asphaltene-related fouling and simultaneously pose catalyst deactivation risks in upgrading units.

In summary, ICP-OES analysis highlights that metal and ash concentrations are fraction-specific and origin-dependent. While aromatics contain minimal impurities, resins and especially asphaltenes act as reservoirs for metals and ash, with EHCO residues being the most problematic. These findings underscore the necessity of targeted dementalization and asphaltene management strategies prior to upgrading or refining EHCO and HCO residues, whereas LCO residues, with their relatively low impurity content, are more favourable feedstocks for catalytic processes.

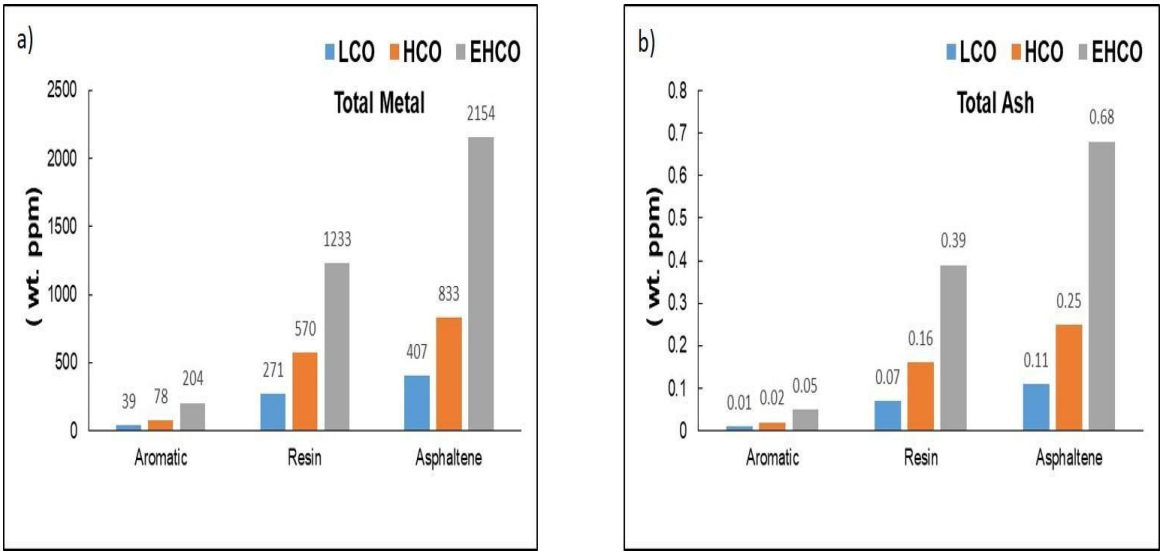


Figure 2.13: Plot showing (a) total metal and (b) ash content in origin-based ARA fractions.

### 2.3.5 Fourier Transfer Infrared Spectroscopy (FTIR)

Infrared spectroscopy (IR) provides valuable qualitative information regarding the hydrocarbon skeleton and functional groups present in crude oil fractions. Despite the complexity of the generated spectra, IR remains a powerful tool for distinguishing functional group variations between fractions and origins, even when absorption bands overlap in regions such as 3600–2600 $cm^{-1}$ (Abdulkadir et al., 2016). The IR spectra of the aromatic fractions from LCO, HCO, and EHCO, shown in Figure 2.14, reveal subtle but meaningful differences in functional group distributions.

In the 3600–2400 $cm^{-1}$ region, associated primarily with O–H stretching vibrations and hydrogen-bonded functional groups, the spectrum for LCO aromatics exhibits a broad band, suggesting the presence of strongly hydrogen-bonded hydroxyl groups. In contrast, HCO aromatics display a sharper peak, indicative of relatively free O–H or N–H stretching modes, while EHCO shows an intermediate response. These variations suggest differences in polar group content and hydrogen bonding environments among the fractions.

Within the 2800–2000 $cm^{-1}$ region, typically attributed to aliphatic C–H stretching and possible overtone/combination bands, distinct differences emerge. Notably, LCO aromatics lack a peak around 2700 $cm^{-1}$, whereas both HCO and EHCO exhibit clear absorptions, suggesting a stronger presence of aliphatic functionalities or aldehydic groups in the latter two. Furthermore, peaks observed at 2314, 2175, and 2006 $cm^{-1}$ in LCO aromatics disappear in HCO but persist faintly in EHCO, possibly indicating the presence of weakly bound carbonyl-containing species, $CO_2$ overtones, or nitrile-type functionalities in LCO and EHCO, but absent in HCO.

In the 2000–1600 $cm^{-1}$ region, associated with C=O stretching and aromatic C=C vibrations, several consistent features appear across all origins. Peaks at 1936, 1859, and 1712 $cm^{-1}$ are common, reflecting conjugated carbonyl and aromatic skeletal vibrations. Interestingly, the peak intensity at 1597 $cm^{-1}$ is most pronounced in EHCO, suggesting enhanced aromatic ring condensation and higher aromaticity compared with LCO and HCO. Similarly, HCO aromatics show enhanced absorption at 1458 and 1373 $cm^{-1}$, which are typically assigned to C–H bending vibrations in aliphatic groups. This indicates a greater contribution of alkyl substituents in HCO aromatics relative to the other samples.

The 1700 $cm^{-1}$ band, associated with carbonyl stretching (C=O), exhibits distinct profiles across origins: LCO and HCO display broad absorptions in the 1640–1800 $cm^{-1}$ range, suggesting a variety of oxygenated species, while EHCO presents a sharp peak, indicating more specific or isolated carbonyl functionalities.

Finally, in the 1400–400 $cm^{-1}$ fingerprint region, the spectra for all three origins show broadly similar patterns, suggesting a common backbone of aromatic skeletal vibrations, C–H out-of-plane bending, and substituted benzene structures. However, subtle variations

in intensity may still reflect differences in substitution patterns and the degree of aromatic condensation.

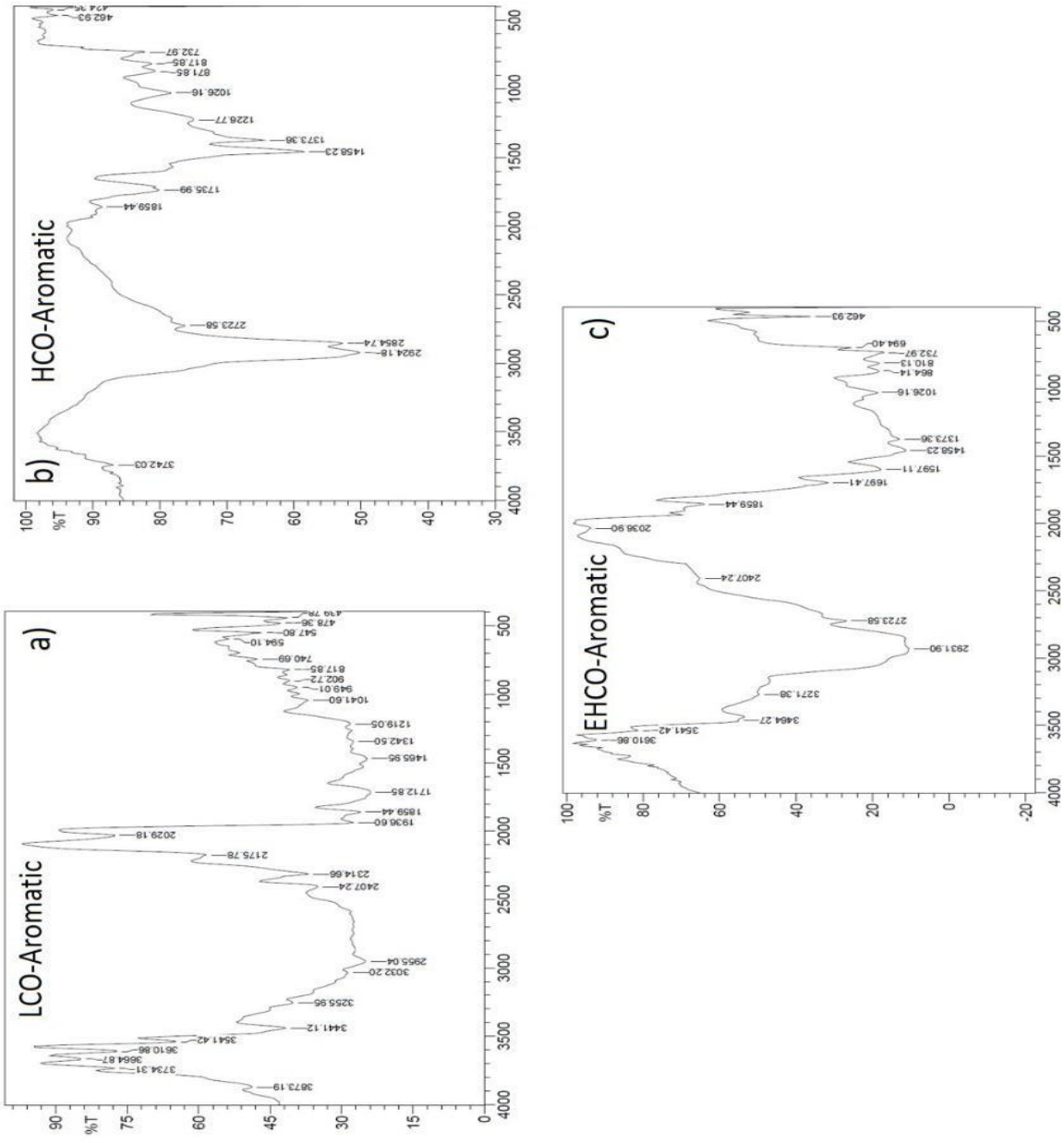


Figure 2.14: FTIR spectra of the studied origin-based aromatics (a) LCO (b) HCO and (c) EHCO

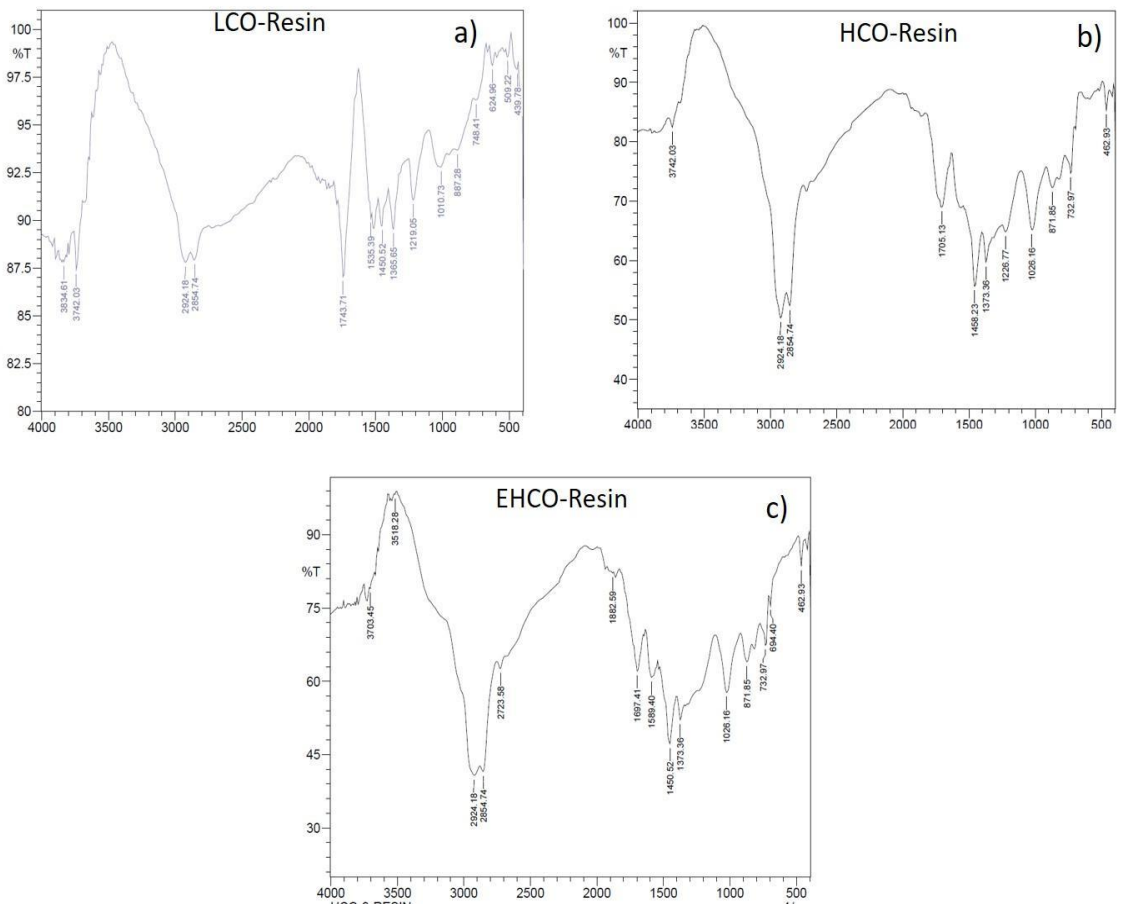


Figure 2.15: FTIR spectra of the studied origin-based resins (a) LCO (b) HCO and (c) EHCO

The FTIR spectra of the vacuum residue fractions provide crucial insights into the presence and distribution of different functional groups. In the 3600–3800 $cm^{-1}$ region, a weak but noticeable absorption corresponding to the O–H stretching vibration of alcoholic groups was observed (Fig. 2.15). This suggests the presence of hydroxyl functionalities, most likely originating from phenolic compounds or alcohol derivatives. Similarly, the absorption band between 3450–3560 $cm^{-1}$, typically attributed to N–H stretching in primary amines, was detected in some fractions; however, it was notably absent in all HCO fractions. This absence indicates a lower concentration or lack of amine-type nitrogen-containing compounds in HCO, in contrast to LCO and EHCO, where nitrogen functionalities are more pronounced.

In the 2800–2950 $cm^{-1}$ region, characteristic absorptions of aliphatic C–H stretching from $CH_2$ and $CH_3$ groups were consistently observed across all samples, reflecting the presence of aliphatic side chains bound to aromatic structures. A minor but distinct aldehydic C–H absorption near 2700 $cm^{-1}$ further confirms the occurrence of oxygenated hydrocarbons, particularly in LCO and EHCO.

Interestingly, LCO and EHCO aromatics exhibited sharp absorptions at 2183 $cm^{-1}$ and 2029 $cm^{-1}$, assigned to C≡C stretching of alkynes and C≡N stretching of nitriles, respectively. These functionalities highlight the occurrence of more complex and unsaturated hydrocarbon species in these origins, whereas such features were absent in HCO.

A strong and broad absorption band was observed in the 1700–1950 $cm^{-1}$ region, which is typically associated with aromatic overtones and conjugated structures. Within this region, more specific bands at 1690–1720 $cm^{-1}$ were identified as signatures of amide, ketone, and ester carbonyl groups. These functional groups were distinctly present in LCO and EHCO asphaltenes but were absent in HCO asphaltenes (Fig. 2.16). This difference reinforces the compositional variability of asphaltenes between origins, where LCO and EHCO contain a greater abundance of oxygenated species compared to the relatively oxygen-deficient HCO.

The 1500–1600 $cm^{-1}$ region displayed strong absorption bands corresponding to C=C stretching vibrations of conjugated alkenes, further confirming the aromatic and olefinic nature of the fractions. In addition, distinct signals observed at 1450–1460 $cm^{-1}$ and 1360–1380 $cm^{-1}$ were attributed to asymmetric and symmetric bending vibrations of methyl and methylene groups, respectively. These bands were consistently present in all asphaltene samples (LCO, HCO, and EHCO), indicating that despite compositional variations, all origins retain aliphatic side chains attached to the aromatic cores.

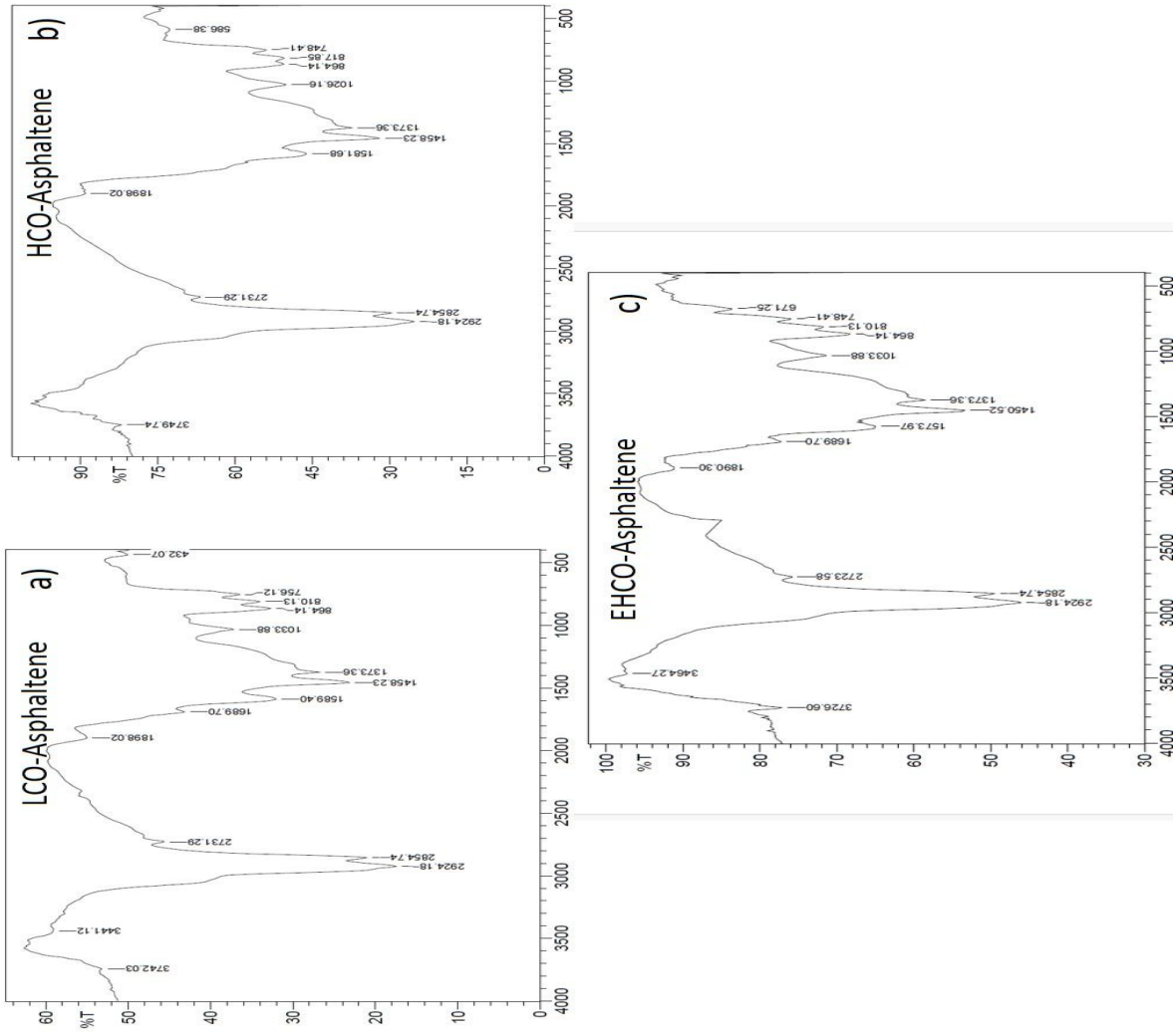


Figure 2.16: FTIR spectra of the origin based asphaltenes (a) LCO (b) HCO and (c) EHCO

The fraction contained bands assigned from 860 to 880 $cm^{-1}$ which was assigned to the vibration of pera or disubstituted aromatic -CH, likewise 810 to 820 $cm^{-1}$ was designated as ortho substituted aromatic -CH , as well 730 to 760 $cm^{-1}$ was assigned to meta substituted aromatic –CH, which were out of plane deformation vibration of aromatic -CH with functional group dependent on the position on the amount of adjacent aromatic -CH atoms in the aromatic framework. Signal appeared for mono substituted aromatic rings between 620 to 680 cm-1: in EHCO asphaltene and resins samples and was absent for -CH peak LCO, and MCO asphaltene and resins. LCO, HCO and MCO aromatic fractions

were absent for -CH peak. It is recognizable that the judgement of the spectrum in the fingerprint region is complicated, as various bands of different functional groups overlap. This extracted an exclusive and definite assignment of all bands in the complex ARA fraction. Therefore, the given functional designations should rather be seen as justification-based recommendations.

The spectra of LCO asphaltene reveal two sharp bands in which one is at about 2924 cm-1 and the other is close to 2854 $cm^{-1}$ (fig. 2.16a). This range is noted for aliphatic C-H stretching that regularly includes strongest bands in the spectra. Hence, these bands for LCO asphaltene are assigned to asymmetric and symmetric stretching of C-H of methylene (Asemani et al., 2020), respectively. Six bands are present within the range 2000 to 1000 cm-1. The small bands at 1898, 1689, 1589, 1458, 1373, and 1033 are assigned to C=O in mixed ketones, C=C in aromatics, scissors C-CH2, C=C in aromatics (ring mode), C-CH3 (umbrella mode) and S=O in alkane substituted sulfoxides. Four bands are identified within the range 1000 to 400 cm-1. The bands at 864, 810, 756 and 432 are allocated to C-H in isolated adjacent hydrogen aromatic rings, in two adjacent hydrogen aromatic rings, in four adjacent hydrogen aromatic rings. For HCO asphaltene, the band positions remain to be similar with not much change. However, a remarkable difference is noticed for EHCO asphaltene when compared with LCO and HCO counterparts. The peak area for bands at 2924 and 2854 cm-1 has decreased significantly.

### 2.3.6 Gel Permeation Chromatography (GPC)

Estimating molecular weight distribution of ARA fractions could be important to anticipate the phase behaviour and prevent asphaltene depositions. Similarly, molecular weight distribution influences the chemical composition which directly affects the combustion characteristics of fuel oil (Saha et al, 2021). Hence determination of molecular weight distribution becomes mandatory which is analysed by Gel Permeation chromatography in the present study. The number-average molecular weight (MN) is defined as the average based on the number of polymer chain molecules at a particular molecular weight, whereas the weight-average molecular weight (MW) corresponds to the mass (or weight) of the polymer chain molecules at a particular molecular weight. Higher side polydispersity indicates the broadness of the molecule. As shown in fig.2.17a, the number-average

molecular weight ($M_N$) of aromatics and resin were basically consistent with those of different origin. However, the $M_N$ of asphaltenes derived from different origins were higher, varying in the range of 2671-4850 ($g.mol^{-1}$). This proposed that the asphaltene, especially derived from HCO, had a larger molecular weight with $M_N$ value of 4850 ($g.mol^{-1}$). Likewise, the weight-average molecular weight (MW) for origin-based ARA fractions based on GPC detection are shown in Fig.2.17b. The results showed that there was a great difference in MW for asphaltene compared with aromatic and resin fraction. The HCO-asphaltene had a high MW value of 21845.

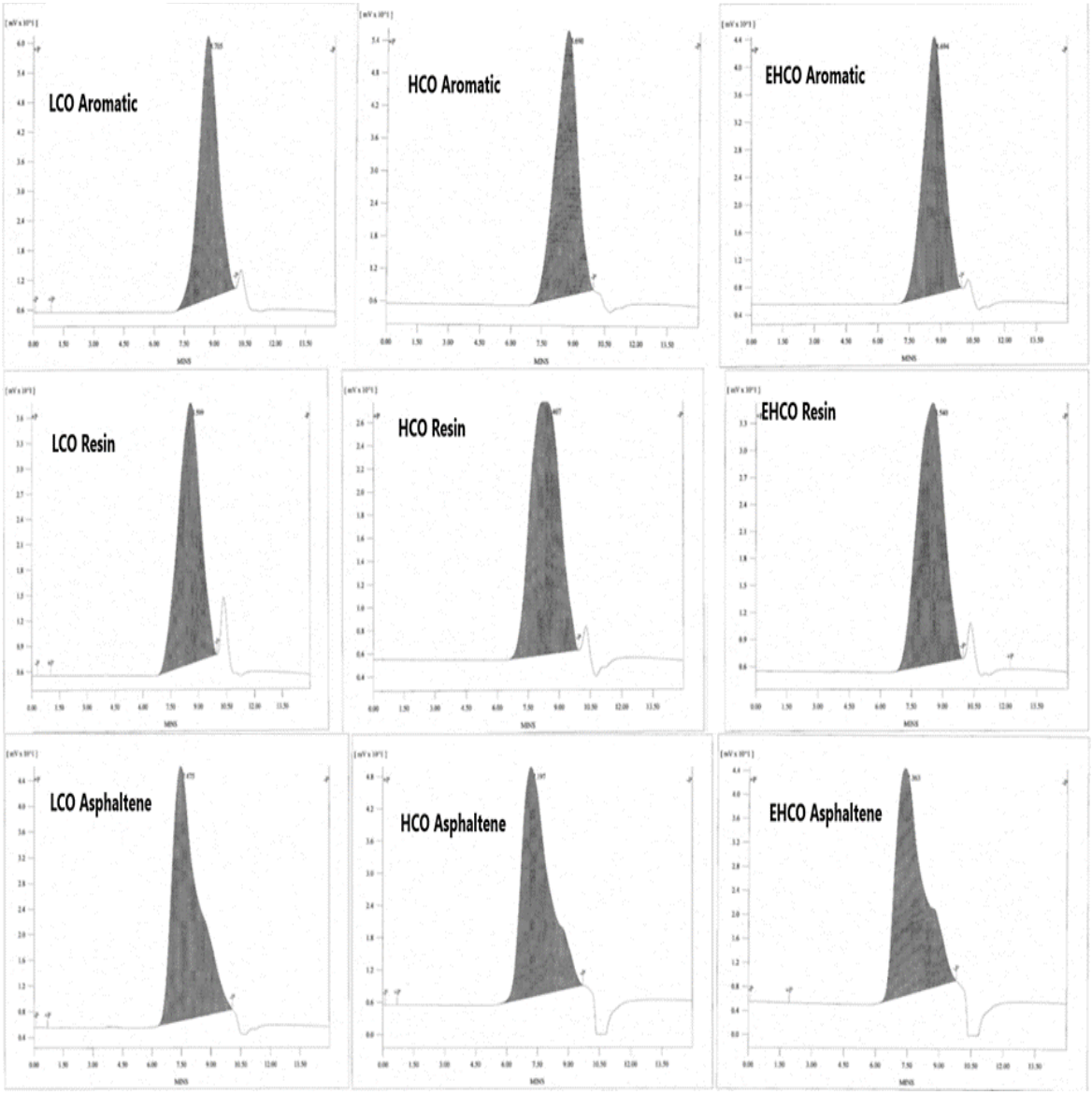


Figure 2.17: Gel Permeation Chromatography of different ARA fraction

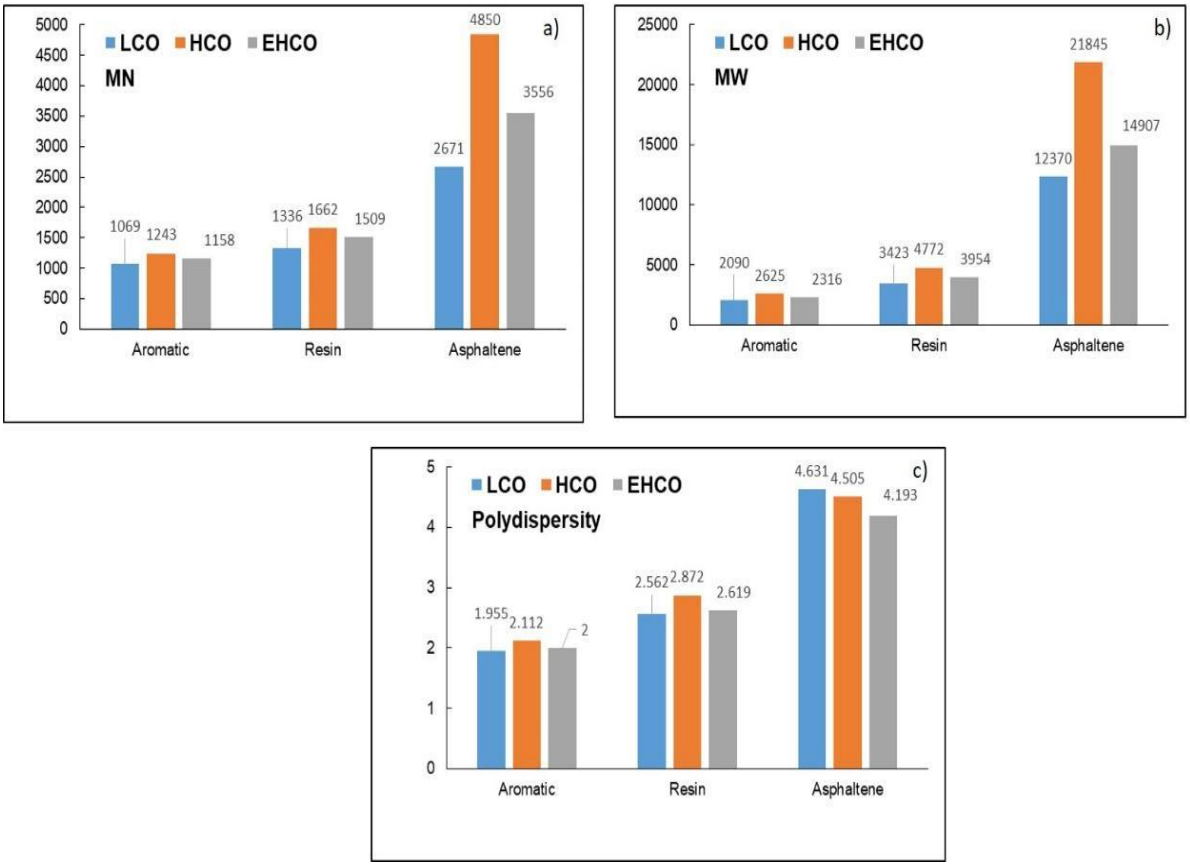


Figure 2.18: Average molecular weight and polydispersity values by GPC (a) MN (b) MW and (c) Polydispersity

The polydispersity, an indication of heterogeneity of a sample based on size from the various fractions, is illustrated in fig.2.18c. The values observed were very similar for the aromatic and resin fractions. Also, it has the same trend as its molecular weight distribution (fig. 2.18a &b). (Mansoori et al, 2021) detected relative values of polydispersity for aromatic, resin and asphaltene from a heavy fraction of crude oil by means of GPC. It is a well reported fact that asphaltenes show a very large size polydispersity. The obtained results reflect the same result. Similarly, the asphaltene fraction has a high polydispersity value as well; it does not follow the trend noticed for molecular weight distribution. For instance, both mass and number molecular weight of asphaltene fraction follows the descending order of HCO, EHCO and LCO. But, for the polydispersity it follows a different order, where LCO has high value followed by HCO and EHCO. G. A. Mansoori

et al. reports broad distribution of sizes and molecular characteristics for asphaltene (Scardaci et al, 2021; Oldham et al. 2022) investigated polydispersity of crude oil due to asphaltene oxidation and hypothesized that increased polydispersity affects viscosity.

### 2.3.7 Nuclear Magnetic Resonance (NMR) spectroscopy

Several researchers have published the application of NMR in the assessment of heavy petroleum fractions. The proton NMR spectroscopy is used for quantitative analysis of paraffinic and aromatic hydrogen, where carbon NMR spectroscopy is used for paraffinic and aromatic carbon atoms. For such complicated molecules, the aliphatic protons participation on a $^{1}H$ NMR spectrum emerges as a large signal with a continuous superimposing of numerous peaks and most strong compared to aromatics and are basically classified into three types of protons namely, a, b and c with reference to an aromatic core. The investigation of the range of every kind is not simple to attain but are commonly resolved from 0.1 to 1.1 ppm for d type protons, broad peck obtained at 1.2 to 2.1 ppm for c type protons, 6.0 to 7.1 ppm for b type protons and 7.0 to 9.0 for a type proton. Proton NMR provides a type of hydrogen and its concentration in compounds and also describes the nature of compounds. Proton NMR attributed δ position of alkyl or paraffinic is 0.1 to 1.1 for methyl, 1.2 to 2.1 for aliphatic methylene and 2.2 to 4.0 for naphthenic or -CH, -$CH_2$ group proton. The aromatic proton resonance δ position for mono aromatic ring 6.0 to 7.1 and di. Tri and tetra or pera aromatic rings 7.3 to 9.0. Where $CDCl_3$ three peaks appeared at 7.26 and TMS at 0. Table 2.12 shows the total aliphatic and aromatic proton. In aromatic, total aliphatic hydrogen increased from light to heavy and total aromatic hydrogen decreased from light to heavy. However, the similar contribution was not found in resins, where heavy crude resins have less aliphatic hydrogen and more aromatic hydrogen as compared to other resins fraction. Asphaltenes fraction have similar aromatic fraction aromatic proton increased from light to heavy and aromatic proton decreased from light to heavy. These results clearly signposted for aromatics and asphaltenes where light to extra heavy aromatic protons decreased and aliphatic protons increased, however the resins did not follow the similar trend also C/H ratio in elemental analysis similar trend was derived. The carbon skeleton was justified by the $^{13}C$ NMR which provided the structure information of carbon compounds discussed in Table 2.13.

For this reason, $^{13}$CNMR spectra has turned out to be a typical choice for the analysis of crude oil fractions.

| NMR | Types | δ position | AROMATIC | | | RESIN | | | ASPHALTENE | | |
|---|---|---|---|---|---|---|---|---|---|---|---|
| | | | LCO | MCO | HCO | LCO | MCO | HCO | LCO | MCO | HCO |
| 1H NMR | Hal; γ | 0,1-1,1 | 18,08 | 22,59 | 21,63 | 17,14 | 18,39 | 17,98 | 33,42 | 17,15 | 22,25 |
| | Hal; β | 1,2-2,1 | 47,65 | 55,03 | 44,54 | 47,00 | 52,01 | 45,55 | 37,83 | 55,50 | 56,07 |
| | Hal; α | 2,2-4,0 | 18,00 | 10,82 | 23,29 | 22,59 | 18,68 | 20,70 | 13,35 | 17,81 | 13,29 |
| | Har mono aromatic rings | 6,0-7,1 | 7,87 | 6,22 | 5,16 | 5,03 | 4,99 | 4,96 | 9,22 | 4,65 | 3,46 |
| | Har of di, tri and tetra aromatic rings | 7,3-9,0 | 8,39 | 5,34 | 5,38 | 8,23 | 5,94 | 10,80 | 6,18 | 4,89 | 4,94 |
| | Total aliphatic hydrogen | 0,4-4,0 | 83,73 | 88,44 | 89,46 | 86,73 | 89,08 | 84,23 | 84,60 | 90,46 | 91,61 |
| | Total aromatic hydrogen | 6,0-9,0 | 16,26 | 11,56 | 10,54 | 13,26 | 10,93 | 15,76 | 15,40 | 9,54 | 8,40 |

Table 2.12: $^{1}$H NMR protons distribution of ARA fractions

When comparing $^{1}$H and$^{13}$C NMR spectra it is plausible to distinguish many variations between them. For instance, $^{13}$C NMR spectra have huge chemical shifts scale (more than 220 ppm) that diminishes over lapping between peaks. The $^{13}$C NMR is insensible than $^{1}$H

NMR because of its reduced natural abundance and magnetogyric ratio of the $^{13}C$ nucleus, but in the event of the $^{1}H$ decoupled $^{13}C$ NMR spectra it is more straightforward when there is no peak splitting. The $^{13}C$ NMR signals between 20.00 and 40.00 ppm come from aliphatic of -CH and -$CH_2$ associated to linear alkanes and cyclic compounds. The methyl group has $^{13}C$ NMR signals 10 to 20 with branches of the methyl group also appearing in this range. While aromatic carbon showed the signal in $^{13}C$ NMR between 110 to 160 ppm. Above table represent the aromatic carbon increasingly pattern showing from light to heavy. However, the total carbon lowers side in HCO fractions matrix due to higher side hetero atoms.

| **NMR** | **Types** | **δ position** | **AROMATIC** | | | **RESIN** | | | **ASPHALTENE** | | |
|---|---|---|---|---|---|---|---|---|---|---|---|
| | | | **LCO** | **MCO** | **HCO** | **LCO** | **MCO** | **HCO** | **LCO** | **MCO** | **HCO** |
| $^{13}C$ NMR | Methyl of carbon to aliphatic or alkyl chain | 10-20 | 11,51 | 13,24 | 3,34 | 12,79 | 8,79 | 8,40 | 7,48 | 13,08 | 4,76 |
| | Methylene of carbon to aliphatic or alkyl chain | 20-25 | 11,51 | 8,68 | 13,04 | 9,30 | 9,56 | 13,20 | 7,48 | 8,41 | 9,52 |
| | Methylene group attached to aromatic ring | 25-40 | 9,71 | 36,53 | 42,14 | 41,67 | 49,35 | 50,80 | 33,18 | 35,98 | 71,43 |
| | CH of aromatic compounds | 110-160 | 67,27 | 41,55 | 41,47 | 36,24 | 32,30 | 27,60 | 51,87 | 42,52 | 14,29 |
| | Total aliphatic carbon | 10-40 | 32,73 | 58,45 | 58,52 | 63,76 | 67,70 | 72,40 | 48,14 | 57,47 | 85,71 |
| | Total aromatic carbon | 110-160 | 67,27 | 41,55 | 41,47 | 36,24 | 32,30 | 27,60 | 51,87 | 42,52 | 14,29 |

Table 2.13: $^{13}C$ NMR protons distribution of ARA fractions.

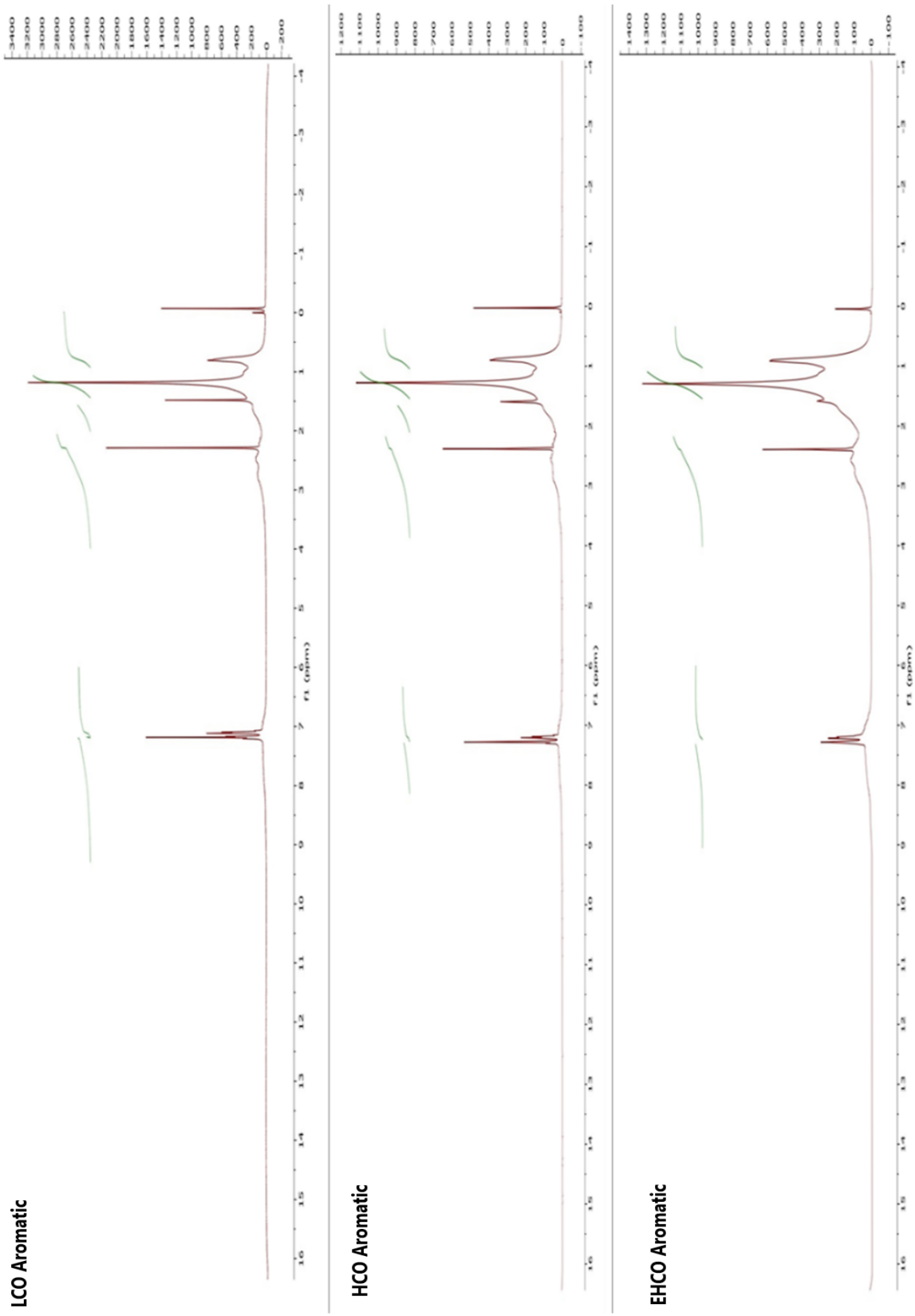


Figure 2.19: $^{1}$H NMR spectra of different aromatics

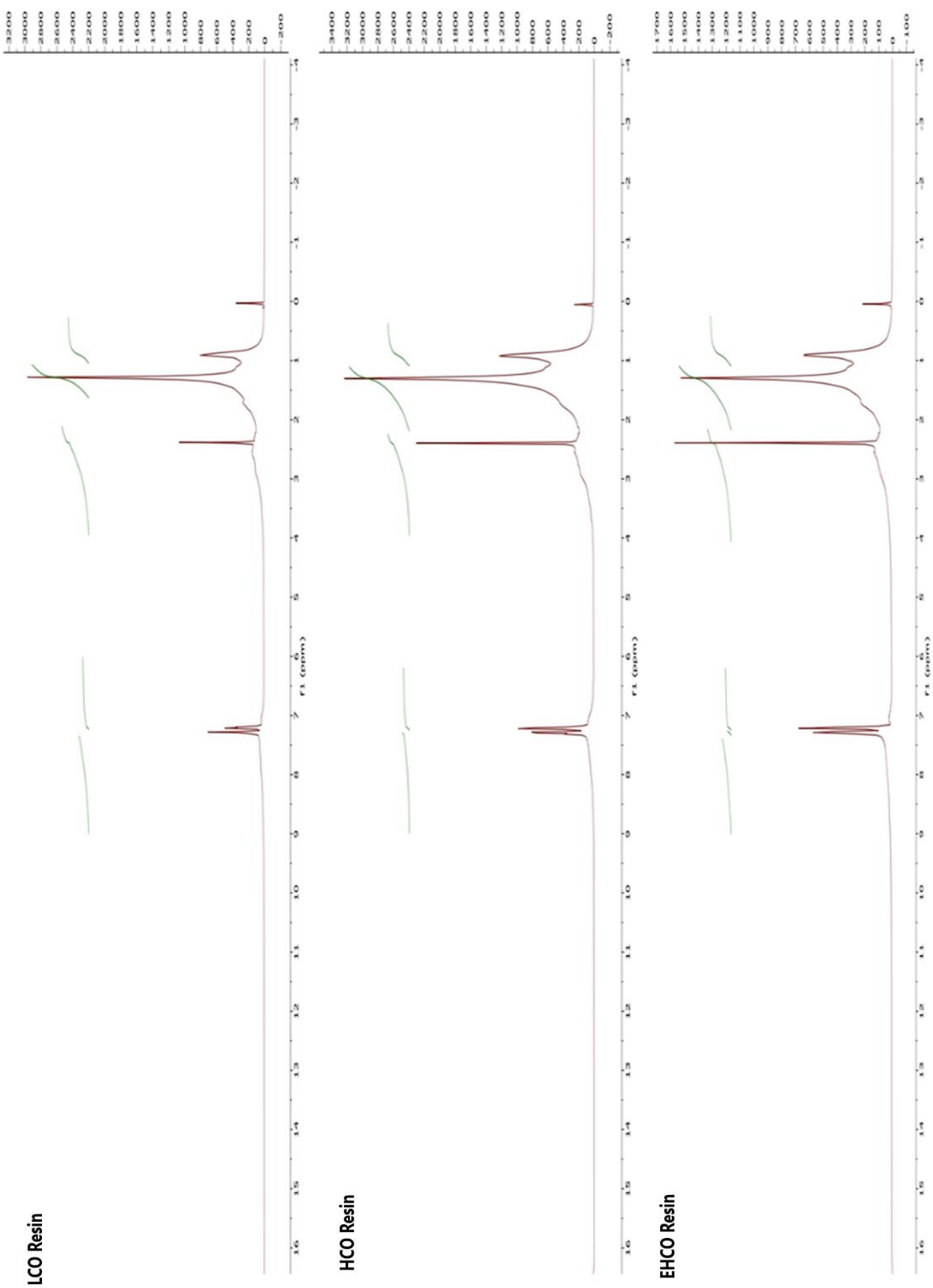


Figure 2.20: 1H NMR spectra of different resins

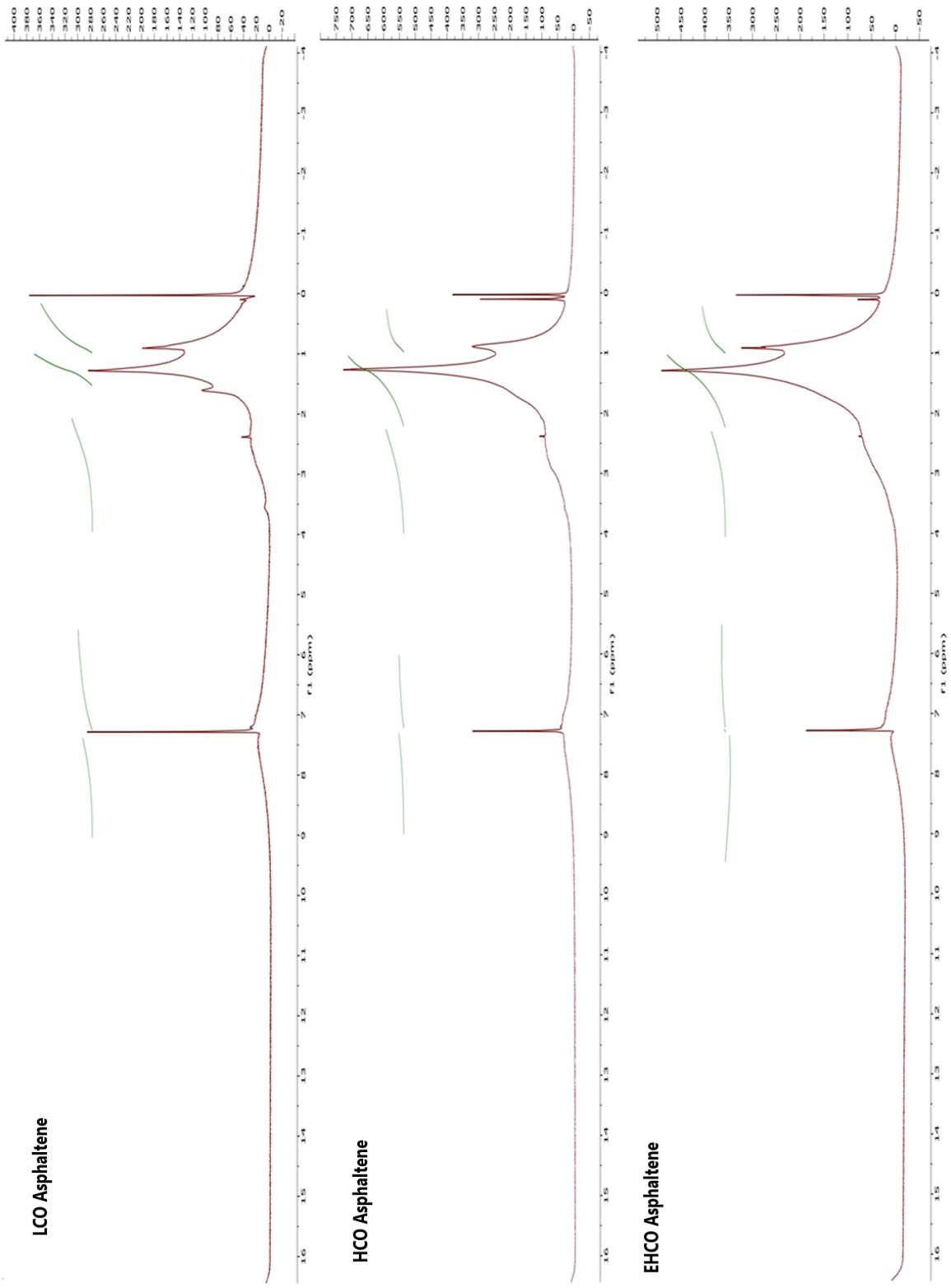


Figure 2.21: 1H NMR spectra of different asphaltenes

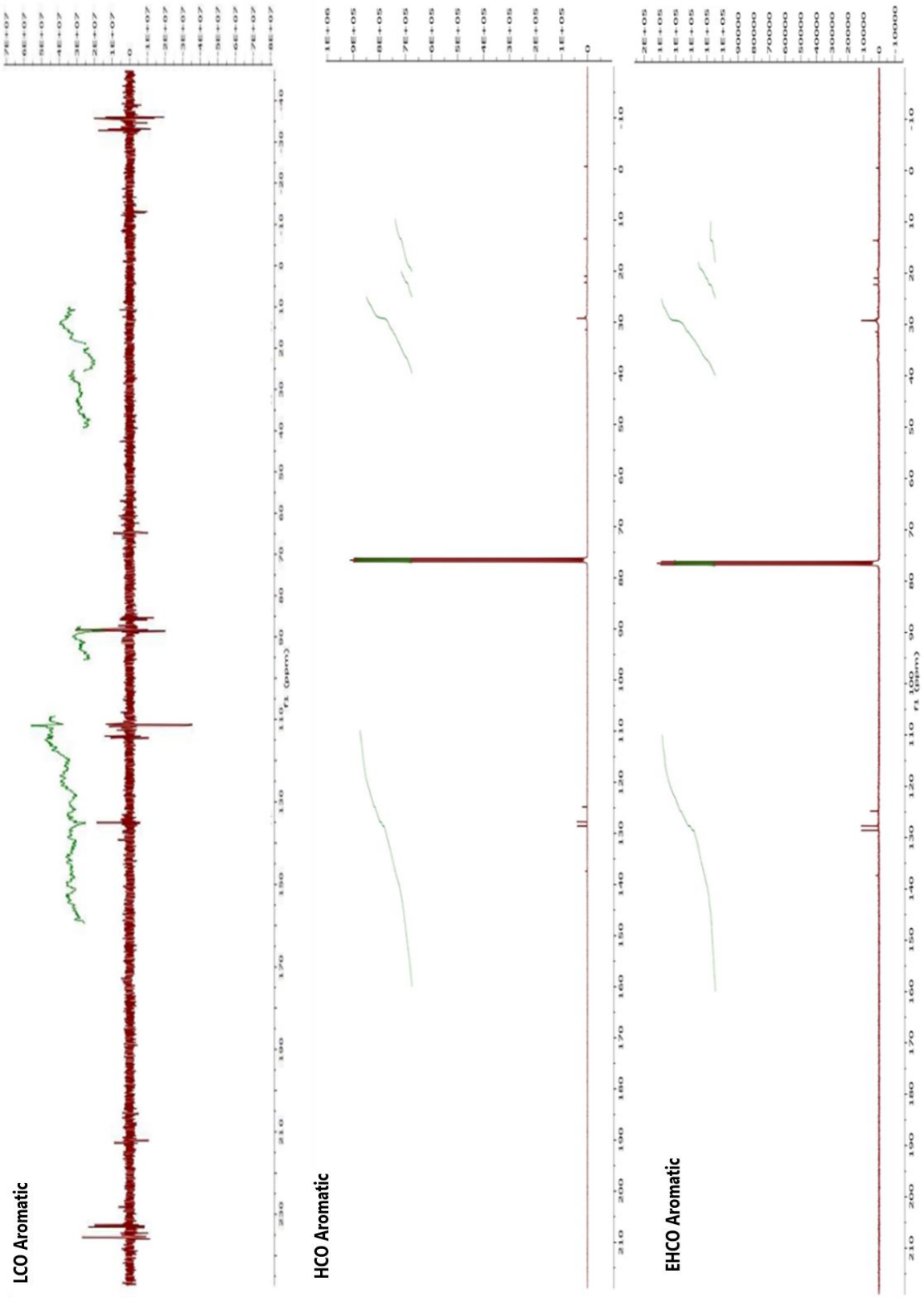


Figure 2.22: 13CNMR spectra of different aromatics

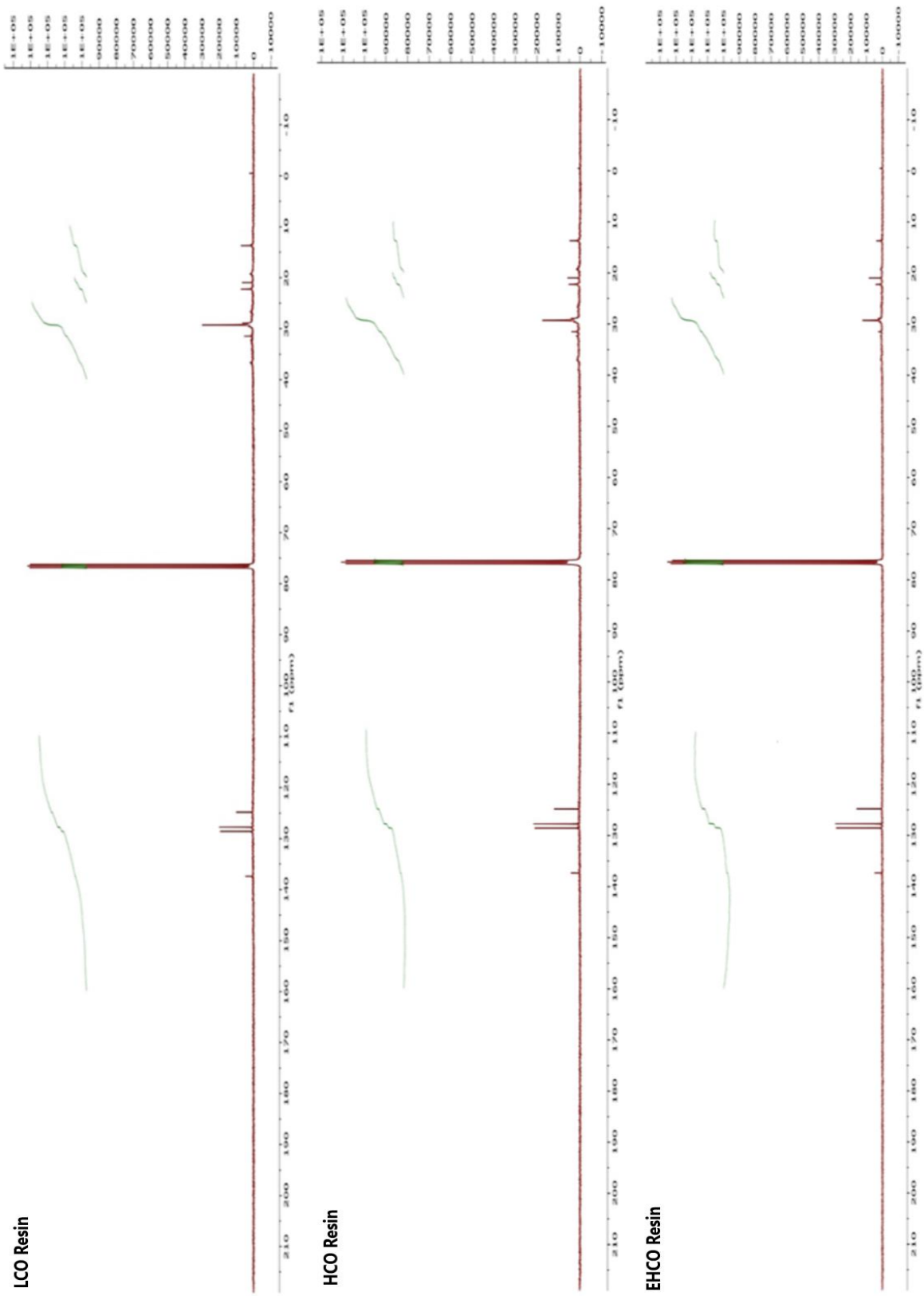


Figure 2.23: 13CNMR spectra of different resins

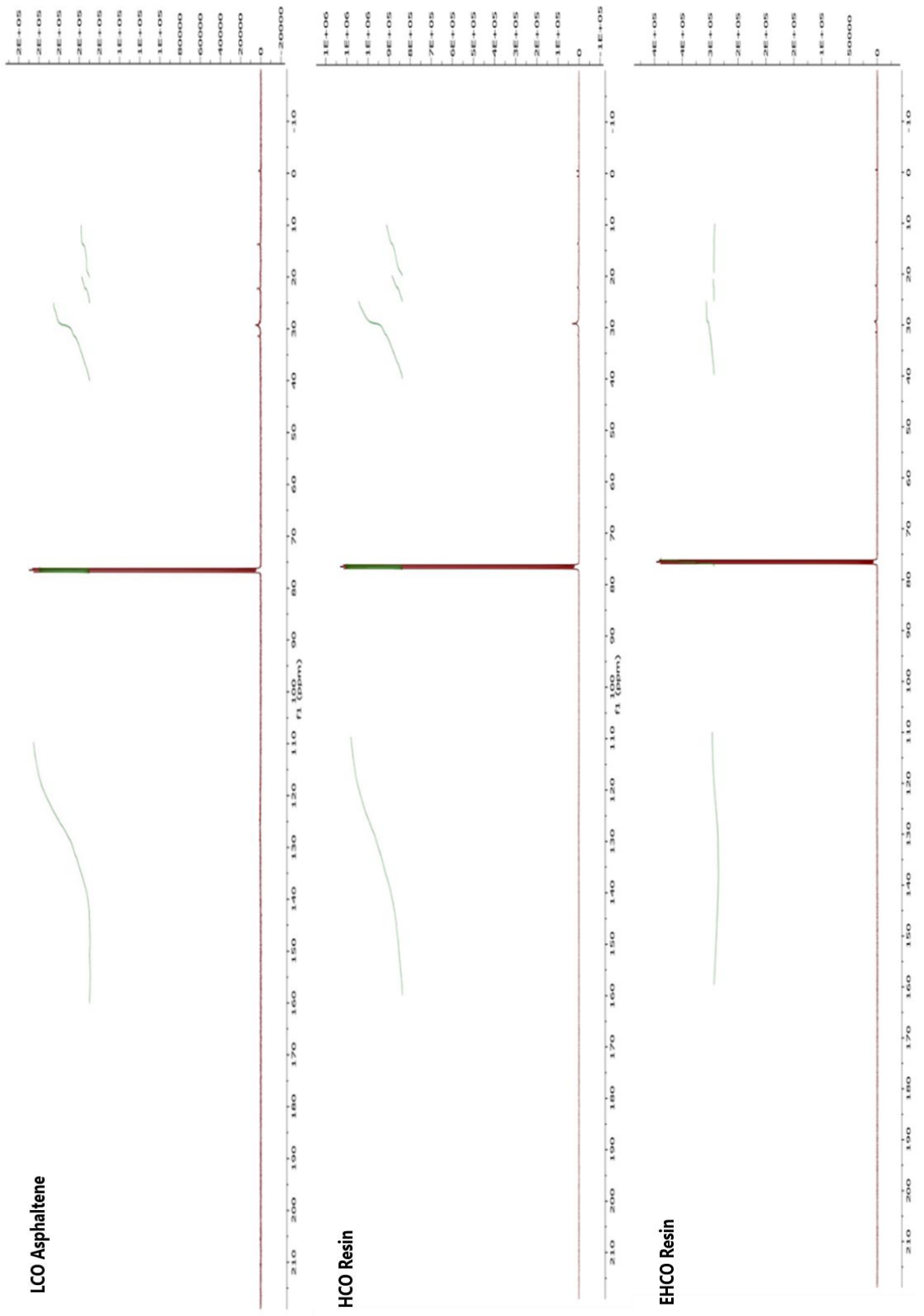


Figure 2.24: 13CNMR spectra of different asphaltenes

## 2.4 Conclusion

The combined FTIR, GPC, and NMR analyses provided comprehensive insights into the structural and molecular features of ARA fractions from different crude oil origins. FTIR spectra confirmed the presence of diverse functional groups, including aliphatic and aromatic C–H, carbonyl, and heteroatom-linked functionalities, with clear substitution patterns in aromatic domains [23,24]. GPC results showed that asphaltenes possess the highest molecular weight and broad polydispersity, especially in HCO fractions, reflecting their structural complexity and aggregation tendencies [25,26]. $^{1}$H NMR analysis indicated a decrease in aromatic protons and an increase in aliphatic protons from light to heavy fractions, whereas $^{13}$C NMR confirmed progressive aromatic carbon enrichment with heteroatom incorporation in heavier fractions [27,28]. Overall, these findings highlight the increasing chemical complexity and heterogeneity of heavier crude fractions, which directly influence asphaltene precipitation, fuel quality, and refining challenges [29]. The complementary application of spectroscopic and chromatographic techniques thus provides a valuable framework for understanding and managing the behaviour of ARA fractions in refining processes [30].

## 2.5 References


1. Bae, E., Kim, S., Kim, S., & Rodgers, R. P. (2011). Characterization of shale oils by Fourier transform ion cyclotron resonance mass spectrometry: Insights into aromatic and heteroatom species. *Energy & Fuels*, *25*(11), 5052–5058. https://doi.org/10.1021/ef201123z
2. Kumar, N., Panda, A. K., & Singh, R. K. (2019). Application of high-resolution mass spectrometry in petroleum and heavy oil analysis. *Fuel*, *235*, 1021–1030. https://doi.org/10.1016/j.fuel.2018.08.131
3. Kumar, S., Rodgers, R. P., Marshall, A. G., & Hsu, C. S. (2013). Advanced mass spectrometry for molecular-level characterization of crude oils and their fractions. *Annual Review of Analytical Chemistry*, *6*(1), 525–549. https://doi.org/10.1146/annurev-anchem-062012-092612
4. Larter, S. R., & Mills, N. (1991). The use of pyrolysis-gas chromatography in petroleum exploration. *Organic Geochemistry*, *17*(6), 823–830. https://doi.org/10.1016/0146-6380(91)90033-G
5. Lee, S., Kim, H., & Cho, Y. (2021). Structural analysis of vacuum residues and heavy oils using advanced nuclear magnetic resonance techniques. *Fuel Processing Technology*, *213*, 106661. https://doi.org/10.1016/j.fuproc.2020.106661
6. Mondello, L., Dugo, G., & Bartle, K. D. (2008). Comprehensive two-dimensional gas chromatography in petroleum and petrochemical analysis. *Journal of Chromatography A*, *1186*(1–2), 2–21. https://doi.org/10.1016/j.chroma.2007.09.089
7. Ramirez, C., Martínez, A., & Lopez, J. (2020). Pyrolysis–GC/MS for characterization of heavy petroleum fractions: Insights into biomarkers and heteroatom compounds. *Journal of Analytical and Applied Pyrolysis*, *149*, 104835. https://doi.org/10.1016/j.jaap.2020.104835
8. Shellie, R. A., Marriott, P. J., & Morrison, P. D. (2016). Comprehensive two-dimensional gas chromatography (GC×GC) and its application to the analysis of petroleum. *Journal of Separation Science*, *39*(1), 73–89. https://doi.org/10.1002/jssc.201500888

9. Silva, R., Pereira, R., & Lucas, E. (2017). Insights into asphaltene and resin structures from NMR spectroscopy. *Energy & Fuels*, *31*(4), 3684–3693. https://doi.org/10.1021/acs.energyfuels.6b02985

11. Wang, X., Zhao, X., & Qian, K. (2019). Characterization of petroleum heavy fractions using ultrahigh-resolution mass spectrometry. *Fuel*, *239*, 1312–1320. https://doi.org/10.1016/j.fuel.2018.11.116
12. Smith, J., Alvarez, D., & Chen, L. (2022). Characterization of sulfur and nitrogen species in vacuum residue oil using API-MS: Positive and negative ion mode studies. *Fuel*, *320*, 123875. https://doi.org/10.1016/j.fuel.2022.123875
13. Zhang, Y., Liu, H., & Zhao, W. (2023). Application of API-MS with solvent extraction and ion exchange for characterization of heteroatomic species in vacuum residue oils. *Energy & Fuels*, *37*(4), 2951–2963. https://doi.org/10.1021/acs.energyfuels.2c03841

13. Liu, H., Yen, T. F., & Wei, J. (1988). Structural characterization of vacuum residues by nuclear magnetic resonance spectroscopy. *Energy & Fuels*, *2*(5), 597–603. https://doi.org/10.1021/ef00011a010
14. Liu, H., Wu, C., & Yen, T. F. (1999). NMR spectroscopic study and modeling of thermal reactivity in vacuum residue oils. *Fuel*, *78*(7), 801–809. https://doi.org/10.1016/S0016-2361(98)00214-5
15. Morgan, T. J., George, A., & Green, J. (2010). Characterization of Maya crude oil by NMR spectroscopy: Implications of sulfur species on refining. *Energy & Fuels*, *24*(5), 3143–3151. https://doi.org/10.1021/ef901234k
16. Hauser, A., Müller, H., & Richter, M. (2014). NMR study of thermal cracking behavior in heavy oils: Focus on oxygen-containing species. *Fuel Processing Technology*, *126*, 178–187. https://doi.org/10.1016/j.fuproc.2014.04.019
17. Garcia, R., Santos, D., & Ramos, A. (2015). Comprehensive NMR analysis of petrochemical residues: Balancing aromatic and aliphatic carbons for refining optimization. *Journal of Petroleum Science and Engineering*, *135*, 507–515. https://doi.org/10.1016/j.petrol.2015.09.018

18. Wang, X., Qian, K., & Zhao, X. (2014). Combined NMR and FT-ICR mass spectrometry for characterization of residual oils: Comparative analysis of vacuum residue and lighter fractions. *Energy & Fuels, 28*(10), 6369–6378. https://doi.org/10.1021/ef501456y
19. Negin, C., Rasekh, H., & Mousavi, S. M. (2016). Application of GC–MS in petroleum residue characterization: A focus on pyrolysis behavior of heavy oils. Fuel Processing Technology, 148, 180–190. https://doi.org/10.1016/j.fuproc.2016.01.020
20. Xu, C., Chen, J., & Guo, H. (2005). Pyrolysis behavior of vacuum residue studied by GC–MS: Evolution of hydrocarbon fractions with temperature. Journal of Analytical and Applied Pyrolysis, 73(1), 13–23. https://doi.org/10.1016/j.jaap.2004.11.003
21. Abutaqiya, M., Singh, R., & Hossain, M. (2019). Comparative pyrolysis of petroleum asphaltenes and bio-asphaltenes using GC–MS. Energy & Fuels, 33(7), 6598–6608. https://doi.org/10.1021/acs.energyfuels.9b01012
22. Nenov, V., Petrova, S., & Ivanov, D. (2020). Characterization of oilfield sludge pyrolysis by GC–MS: Volatile release and hydrocarbon breakdown. Waste Management, 102, 362–370. https://doi.org/10.1016/j.wasman.2019.10.044
23. Shi, B., Zhang, X., & Wang, J. (2010). Identification of high-molecular-weight polycyclic aromatic hydrocarbons in vacuum residue oils by GC–MS. *Fuel, 89*(12), 3725–3733. https://doi.org/10.1016/j.fuel.2010.07.012
24. Lee, D., Park, S., & Kim, H. (2022). High-performance liquid chromatography analysis of polycyclic aromatic hydrocarbons in heavy oils: Sensitivity for low-molecular-weight PAHs. *Journal of Chromatography A, 1663*, 462760. https://doi.org/10.1016/j.chroma.2022.462760
25. Zhang, L., Chen, Y., & Zhao, H. (2023). Molecular characterization of oxygenated polycyclic aromatic hydrocarbons in vacuum residue oils using LC–MS. *Fuel, 342*, 127895. https://doi.org/10.1016/j.fuel.2023.127895
36. Gomez, R., Torres, M., & Fernandez, J. (2020). Selective detection of high-ring polycyclic aromatic hydrocarbons in petroleum residues using fluorescence

spectroscopy. *Journal of Petroleum Science and Engineering*, *195*, 107885. https://doi.org/10.1016/j.petrol.2020.107885

37. Wang, X., Li, P., & Zhang, Q. (2019). High-resolution analysis of polycyclic aromatic hydrocarbons in heavy oils by FT–ICR MS. *Energy & Fuels*, *33*(6), 5312–5323. https://doi.org/10.1021/acs.energyfuels.9b00215
38. Choi, J., Park, H., & Kim, S. (2022). Metal–organic and covalent organic frameworks as emerging catalysts for hydrocarbon and biomass conversion. *Applied Catalysis B: Environmental*, *310*, 121297. https://doi.org/10.1016/j.apcatb.2022.121297
39. Nie, L., Yu, J., Jaroniec, M., & Chen, X. (2020). Enhanced catalytic performance of transition metal oxides through the control of oxygen vacancies. *Chemical Society Reviews*, *49*(2), 667–699. https://doi.org/10.1039/C9CS00713E
40. Abutaqiya, M., Khan, Z., & Rahman, A. (2019). Green synthesis of nanomaterials for catalytic applications in petroleum refining. *Journal of Cleaner Production*, *236*, 117619. https://doi.org/10.1016/j.jclepro.2019.117619
41. Moy, D., Park, J., & Lee, J. (2013). Hydrocracking of heavy oil fractions using Pd/Hβ zeolite catalyst under mild conditions. *Fuel Processing Technology*, *116*, 123–132. https://doi.org/10.1016/j.fuproc.2013.05.014
42. Speight, J. G. (2020). *Handbook of Petroleum Analysis* (2nd ed.). Wiley.
43. Ali, M. F., & Abbas, S. (2006). A review of methods for the demetallization of residual fuel oils. *Fuel Processing Technology*, *87*(7), 573–584. https://doi.org/10.1016/j.fuproc.2005.08.004
44. Boss, C. B., & Fredeen, K. J. (2004). *Concepts, Instrumentation and Techniques in Inductively Coupled Plasma Optical Emission Spectrometry*. PerkinElmer.
45. Mandlate, J. S., et al. (2017). Determination of chlorine and sulfur in crude oil by ICP-OES after microwave-induced combustion. *Journal of Analytical Atomic Spectrometry*, *32*(11), 2125–2133.
46. Santos, M. C., et al. (2018). Advances in microwave-induced combustion for petroleum analysis. *Talanta*, *182*, 316–323.
47. Arenaz-Díaz, M. A., et al. (2017). Microwave-induced combustion for trace element determination in heavy petroleum fractions. *Fuel*, *210*, 167–173.

48. Farmani, M., et al. (2019). Metal and sulfur determination in crude oil using ICP-OES coupled with chemiluminescence detection. *Energy & Fuels*, *33*(6), 5490–5498.
49. Canan, S. S., et al. (2022). Rapid characterization of crude oil by NMR relaxation with user-friendly software. Energy & Fuels, 36(5), 2401–2412.
50. Gao, J., et al. (2020). Molecular characterization of crude oil by $^{1}H$ and $^{13}C$ NMR spectroscopy: Implications for oil source and maturity. Organic Geochemistry, 142, 103995.
51. Rakhmatullin, R., et al. (2020). Qualitative and quantitative analysis of heavy crude oils and their SARA fractions using $^{13}C$ NMR. Fuel, 269, 117352.
52. Morgan, T. J., et al. (2010). Structural characterization of Maya crude oil maltenes and asphaltenes by NMR and laser desorption–mass spectrometry. Energy & Fuels, 24(6), 3380–3387.
53. Rakhmatullin, R., et al. (2018). Detailed $^{13}C$ NMR study of heavy crude oils and SARA fractions. Journal of Petroleum Science and Engineering, 165, 231–239.
54. Chukwuneke, J. L., et al. (2021). Gel permeation chromatography (GPC): Principles, applications, and recent developments. Journal of Analytical Science and Technology, 12(1), 45–59.
55. Merdrignac, I., et al. (2007). Characterization of heavy oils and residues by size exclusion chromatography. *Energy & Fuels, 21*(2), 1024–1030.
56. Verstraete, J., et al. (2010). Advances in size exclusion chromatography for heavy oil analysis. *Fuel, 89*(10), 2723–2730.
57. Nikookar, M., et al. (2022). Molecular weight distribution analysis of asphaltenes and heavy fractions using GPC. *Journal of Petroleum Science and Engineering, 208*, 109624.
58. Azinfar, B., et al. (2019). Characterization of heavy crude oils and residues using combined GPC and simulated distillation. *Fuel, 245*, 274–284.
59. Sarowha, S., et al. (2018). Determination of molecular weights of petroleum products by gel permeation chromatography. *Petroleum Science and Technology, 36*(7), 503–512.

60. Alawani, A., et al. (2020). Characterization of crude oils using GPC and mass spectrometry. *Fuel Processing Technology*, *210*, 106584.
61. Asemani, M., et al. (2020). Structural characterization of crude oil asphaltenes using FTIR spectroscopy. *Fuel, 269*, 117085.
62. Esmaeilian, A., et al. (2023). Comprehensive characterization of asphaltenes using FTIR, NMR, ICP-OES, MS, XRD, and computational chemistry. *Energy & Fuels*, *37*(2), 1021–1036.
63. Melendez, A., et al. (2012). Prediction of SARA fractions in Colombian crude oils by ATR-FTIR spectroscopy and chemometric analysis. *Fuel, 100*, 38–43.
64. Yang, Z., et al. (2022). Data-driven prediction of crude oil properties by integrating FTIR spectroscopy and machine learning approaches. *Journal of Petroleum Science and Engineering*, *210*, 110021.